JOURNAL OF PETROLOGY | VOLUME 50 | NUMBER 6 | PAGES 989–1023 | 2009 | doi:10.1093/petrology/egp029

Geochemical Evolution of Intraplate Volcanism at Banks Peninsula, New Zealand: Interaction Between Asthenospheric and Lithospheric Melts

CHRISTIAN TIMM[1]*, KAJ HOERNLE[1], PAUL VAN DEN BOGAARD[1], ILYA BINDEMAN[2] AND STEVE WEAVER[3]

[1]IFM-GEOMAR LEIBNIZ INSTITUTE OF MARINE SCIENCES, WISCHHOFSTR. 1–3, 24148 KIEL, GERMANY

[2]DEPARTMENT OF GEOLOGICAL SCIENCES, 1272 UNIVERSITY OF OREGON, EUGENE, OR 97403, USA

[3]DEPARTMENT OF GEOLOGICAL SCIENCES, UNIVERSITY OF CANTERBURY, PRIVATE BAG 4800, CHRISTCHURCH, NEW ZEALAND

RECEIVED APRIL 14, 2008; ACCEPTED APRIL 30, 2009
ADVANCE ACCESS PUBLICATION JUNE 24, 2009

Intraplate volcanism was widespread and occurred continuously throughout the Cenozoic on the New Zealand micro-continent, Zealandia, forming two volcanic endmembers: (1) monogenetic volcanic fields; (2) composite shield volcanoes. The most prominent volcanic landforms on the South Island of New Zealand are the two composite shield volcanoes (Lyttelton and Akaroa) forming the Banks Peninsula. We present new $^{40}Ar/^{39}Ar$ age and geochemical (major and trace element and Sr–Nd–Pb–Hf–O isotope) data for these Miocene endmembers of intraplate volcanism. Although volcanism persisted for ~7 Myr on Banks Peninsula, both shield volcanoes primarily formed over an ~1 Myr interval with small volumes of late-stage volcanism continuing for ~1·5 Myr after formation of the shields. Compared with normal Pacific mid-ocean ridge basalts (P-MORB), the low-silica (picritic to basanitic to alkali basaltic) Akaroa mafic volcanic rocks (9·4–6·8 Ma) have higher incompatible trace element concentrations and Sr and Pb isotope ratios but lower $\delta^{18}O$ (4·6–4·9) and Nd and Hf isotope ratios than ocean island basalts (OIB) or high time-integrated U/Pb HIMU-type signatures, consistent with the presence of a hydrothermally altered recycled oceanic crustal component in their source. Elevated CaO, MnO and Cr contents in the HIMU-type low-silica lavas, however, point to a peridotitic rather than a pyroxenitic or eclogitic source. To explain the decoupling between major elements on the one hand and incompatible elements and isotopic compositions on the other, we propose that the upwelling asthenospheric source consists of carbonated eclogite in a peridotite matrix. Melts from carbonated eclogite generated at the base of the melt column metasomatized the surrounding peridotite before it crossed its solidus. Higher in the melt column the metasomatized peridotite melted to form the Akaroa low-silica melts. The older (12·3–10·4 Ma), high-silica (tholeiitic to alkali basaltic) Lyttelton mafic volcanic rocks have low CaO, MnO and Cr abundances suggesting that they were at least partially derived from a source with residual pyroxenite. They also have lower incompatible element abundances, higher fluid-mobile to fluid-immobile trace element ratios, higher $\delta^{18}O$, and more radiogenic Sr but less radiogenic Pb–Nd–Hf isotopic compositions than the Akaroa volcanic rocks and display enriched (EMII-type) trace element and isotopic compositions. Mixing of asthenospheric (Akaroa-type) melts with lithospheric melts from pyroxenite formed during Mesozoic subduction along the Gondwana margin and crustal melts can explain the composition of the Lyttelton volcano basalts. Two successive lithospheric detachment/delamination events in the form of Rayleigh–Taylor instabilities could have triggered the upwelling and related decompression melting leading to the formation of the Lyttelton (first, smaller detachment event) and Akaroa (second, more extensive detachment event) volcanoes.

KEY WORDS: *intraplate volcanism; $^{40}Ar/^{39}Ar$ dating; major and trace element and Sr–Nd–Pb–Hf–O isotope geochemistry; peridotite and pyroxenite melting; lithospheric detachment/delamination*

*Corresponding author. Telephone: +49-431-600-2141. Fax: +49-431-600-2924. E-mail: ctimm@ifm-geomar.de

INTRODUCTION

During the Early Cretaceous, the New Zealand microcontinent, Zealandia, was located at the northern to northwestern margin of the former super-continent Gondwana. Throughout the Mesozoic, before separation from Gondwana, Zealandia experienced voluminous, subduction-related magmatism (Muir *et al.*, 1998). After separation from western Antarctica at ~84 Ma (Waight *et al.*, 1998; Davy, 2006), Zealandia drifted ~6000 km (~70 km/Ma) NW to its present position. The products of intraplate volcanism are ubiquitous in New Zealand and formed nearly continuously throughout the Late Cretaceous and Cenozoic. Widely dispersed monogenetic volcanic fields represent one endmember-type of volcanism, defining broad areas where volcanic activity in some cases lasted tens of millions of years, such as the Waipiata volcanic field in Otago (Coombs *et al.*, 1986; Weaver & Smith, 1989; Hoernle *et al.*, 2006). These fields are characterized by highly to moderately silica-undersaturated volcanic rocks (with small proportions of more evolved differentiates) occurring as small cones, lava flows, pyroclastic deposits, dike intrusions or pillow lavas. The second volcanic endmember is represented by larger composite shield volcanoes, such as the Dunedin and Banks Peninsula volcanoes (Fig. 1).

The most widely accepted explanations for continental intraplate volcanism include the plume hypothesis (Morgan, 1971) and major continental extension and thinning associated with continental rifting and breakup (e.g. Weaver & Smith, 1989). The Lyttelton (NW) and Akaroa (SE) composite shield volcanoes on Banks Peninsula are not associated with a larger age-progressive trend of volcanism in the direction of plate motion, which is inconsistent with the classical plume hypothesis. In addition, seismic tomography data show no evidence for a shallow plume-like thermal anomaly beneath Banks Peninsula, or nearby (e.g. Montelli *et al.*, 2006). Using the current plate motion of ~61 mm/yr (Clouard & Bonneville, 2005), it is difficult to explain the occurrence of volcanism over ~7 Myr in such a restricted area (~90 km by 90 km), as the plate would have drifted ~400 km during this time. In respect to continental extension, the predominant tectonic stress regime in the late Miocene was compressional (Sutherland, 1995). Although an increased rate of rotational deformation and crustal thinning between 25 and 8 Myr ago (Eberhart-Phillips & Bannister, 2002; Hall *et al.*, 2004) may have caused mild local extension, there is no evidence for major lithospheric extension and rifting during the Cenozoic, which could account for the generation of the voluminous amounts of magma required to form the shield volcanoes.

Alternative models for generating the intraplate Cenozoic volcanism on Banks Peninsula include melting of volatile-rich lithosphere (Finn *et al.*, 2005; Panter *et al.*, 2006) and decompression melting of upwelling asthenosphere as a result of lithospheric removal or detachment (Hoernle *et al.*, 2006). To generate extensive melting to form shield volcanoes solely within the lithospheric mantle, a large amount of thermal energy needs to be applied to the base of the lithosphere. In the absence of evidence for a mantle plume or other large thermal anomalies beneath Banks Peninsula, it is unlikely that lithospheric melting can be the sole (major) mechanism for generating the Banks volcanism.

Lithospheric removal is an alternative model for causing Cenozoic volcanism. To explain the intraplate volcanism in the Otago Province of New Zealand, Hoernle *et al.* (2006) noted that the Zealandia lithosphere was exposed to extensive subduction-related fluids and melts while it was located at the northern margin of Gondwana during the Mesozoic. As a result, the lithosphere beneath Zealandia was refertilized, leading to an increase in density (in particular in the deepest portions) relative to the underlying asthenosphere. Being negatively buoyant, the lower lithosphere therefore forms a gravitationally unstable layer, which can detach as Rayleigh–Taylor instabilities. Following lower lithospheric removal, less dense, hot asthenospheric mantle streams up into the resulting gaps in the base of the lithosphere, partially melting as a result of decompression. The upwelling asthenosphere can also trigger melting in the metasomatized base of the lithosphere and asthenospheric melts can interact extensively with the metasomatized (volatile-rich) lithospheric mantle and local continental crust. Lithospheric removal could also explain the fairly thin continental lithosphere (including crust and mantle) beneath Zealandia, which generally ranges between 70 and 100 km but thickens to >150 km beneath the Southern Alps (Stern *et al.*, 2002; Liu & Bird, 2006).

To better understand the temporal, petrological and geochemical evolution of the Banks Peninsula volcanism, we present new $^{40}Ar/^{39}Ar$ ages and a comprehensive geochemical (major and trace element and Sr–Nd–Pb–Hf–O isotope) dataset. Our study is consistent with the Banks volcanism being related to two major lithosphere removal events and serves as a case study for the origin of intraplate volcanism, particularly composite shield volcanoes, on Zealandia.

GEOLOGICAL BACKGROUND

The Lyttelton and Akaroa composite shield volcanoes, located on Banks Peninsula on the east coast of the South Island of New Zealand, have diameters of ~25 km^2 and ~35 km^2, respectively (Fig. 1). The volcanoes were active during the Mid- to Late Miocene (~12–6 Ma, based on K/Ar and Rb/Sr ages; Barley & Weaver, 1988; Stipp & Mc Dougall, 1968; Barley *et al.*, 1998) and represent highly

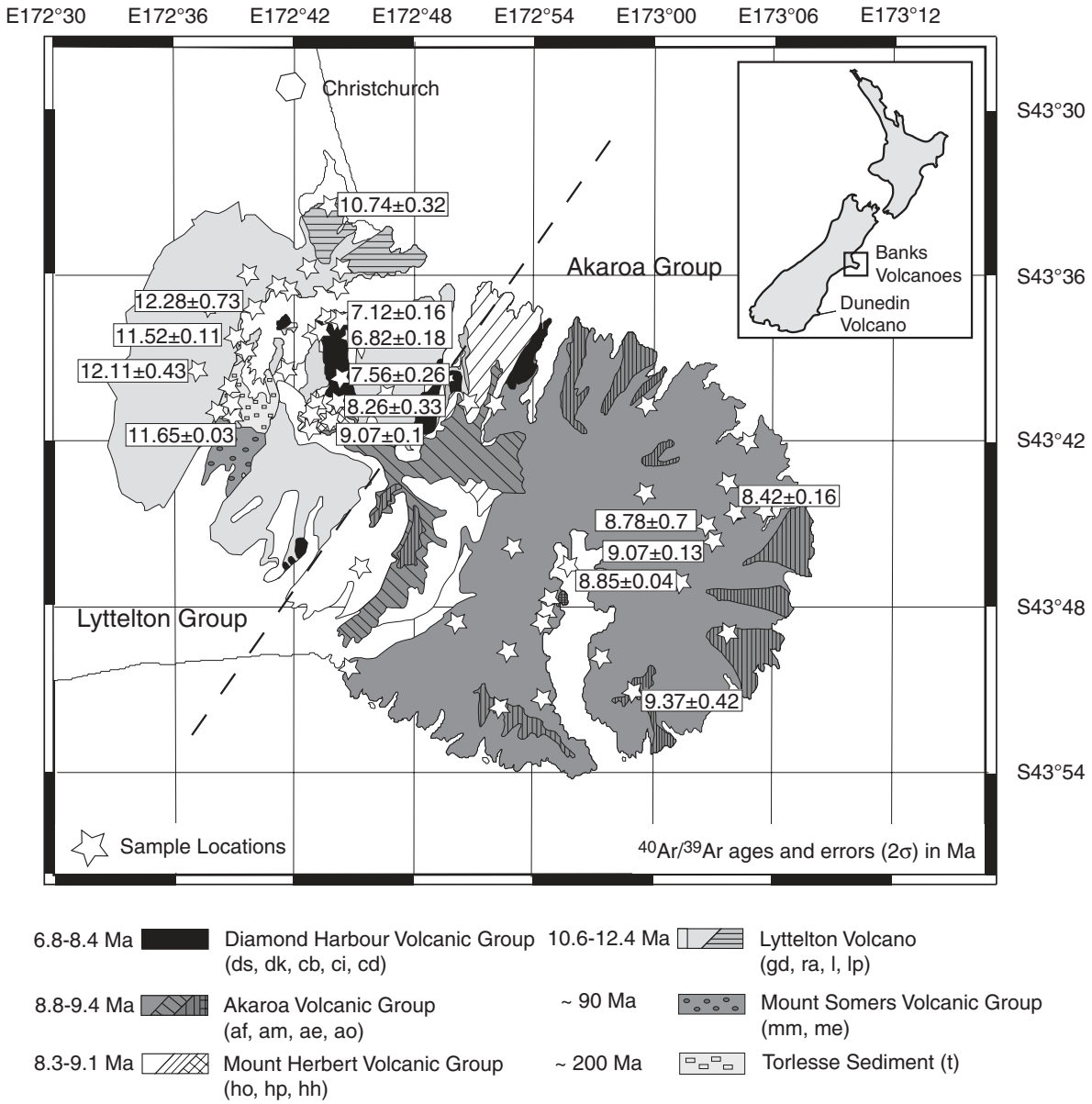

Fig. 1. Simplified geological map of Banks Peninsula, showing the units of the Lyttelton volcano in the NW and the units of the Akaroa volcano in the SE. The Mount Herbert Volcanic Group overlies the Lyttelton volcanic rocks but has a similar age to the Akaroa volcanic rocks. The Diamond Harbour Volcanic Group crops out over the flanks of Lyttelton volcano with the exception of two occurrences on the slopes of Akaroa volcano. Stars mark sample locations and the numbers are $^{40}Ar/^{39}Ar$ ages in Ma with 2σ errors (see Table 1 and Supplementary File 1). The dashed line separates the two composite shield volcanoes, the Lyttelton and Akaroa volcanoes, and also represents a chemical boundary between high-silica Lyttelton and low-silica Akaroa lavas.

eroded remnants of much larger volcanoes. Sector collapse and subsequent erosion allowed the sea to reach the central parts of both volcanoes, forming well-protected natural harbours. Therefore it is ultimately the presence of the Lyttelton volcano, specifically its harbour, that contributed to Christchurch becoming the largest city on the South Island of New Zealand. The Lyttelton volcano sits on Permian–Triassic Torlesse sedimentary rocks of the Rakaia Terrane and on intermediate to silicic, Late Cretaceous volcanic rocks of the Mount Somers Volcanic Group. Drilled lavas, offshore of Banks Peninsula and beneath the surrounding Canterbury Plains, suggest that the shield volcanoes had original diameters of ~35 km for Lyttelton and ~50 km for Akaroa (Weaver & Smith, 1989). A minimum estimate for the volume of the Banks Peninsula volcanic rocks is ~1750 km^3: ~350 km^3 for Lyttelton volcano, ~1200 km^3 for Akaroa volcano and ~200 km^3 for the Mount Herbert and Diamond Harbour

Volcanic Groups on and around the two volcanoes. During the early years of activity, the two coalescing volcanoes formed an island, which became connected to the mainland of the South Island through accumulation of gravel outwash on the Canterbury Plains derived from the nearby Southern Alps mountain ranges (Liggett & Gregg, 1965; Weaver & Smith, 1989).

Based on the stratigraphy established by Sewell *et al.* (1992), the Miocene volcanic activity of the Lyttelton volcano began with the eruption of the undifferentiated Lyttelton Group lavas (map unit l; Fig. 1), which formed the main basaltic shield of the Lyttelton volcano between ~12 and 11 Ma (based on Rb/Sr ages after Barley & Weaver, 1988). Contemporaneously, the Allandale Rhyolite (ra) and the Governors Bay Formation (gb) erupted at ~11 Ma (Barley & Weaver, 1988), whereas a late-stage phase of volcanic activity formed the younger Mt. Pleasant Formation lavas (lp) between ~10·5 and 10 Ma, which directly overlie the undifferentiated Lyttelton Group on the northeastern and southern flanks. Also during the eruption of the shield-building lavas, a radial dike swarm of mafic to felsic rock types was emplaced (Shelley, 1988). The main cone of the Lyttelton volcano at the end of the shield stage probably reached a height of ~1500 m above sea level (Stipp & Mc Dougall, 1968). At ~10 Ma volcanic activity ceased at the Lyttelton volcano and shifted towards the SE. The eruption of the Mount Herbert lavas [including the Orton Bradley (ho) and Port Levy Formations (hp) and the Herbert Peak Hawaiite (hh)] took place initially through vents in the crater of the Lyttelton volcano in subaqueous to water-saturated conditions as indicated by crater-lake deposits (K/Ar ages of 9·5–8 Ma; Weaver & Smith, 1989). Although the Mount Herbert Volcanic Group lavas constitute relatively minor extrusive volumes compared with the Lyttelton and Akaroa volcanoes, they crop out at present at the highest elevations on the Banks Peninsula, with Mount Herbert reaching a height of ~920 m.

Volcanic activity at Akaroa volcano began at ~9 Ma with the eruption of the Tikao Trachyte (ai), contemporaneously with the emplacement of the shield-building lavas of the French Hill Formation (af) between 9·1 and 8·3 Ma (Stipp & Mc Dougall, 1968). The only plutonic rocks on Banks Peninsula are the Duvauchelle Gabbro (ad) and the Onawne Syenite (ao), which occur at or near the Onawne Peninsula in the center of the Akaroa volcano. The stratigraphically younger Mt Sinclair (am) and Te Oka Formations (ae) directly overlie the French Hill Formation at the northern, western and southwestern flanks of the Akaroa volcano (K/Ar ages of 8·6–8·0 Ma after Stipp & Mc Dougall, 1968). The shield of the Akaroa volcano probably reached a height of >1800 m above sea level in the past (Liggett & Gregg, 1965). Mafic and felsic dikes also occur in the intrusive core of the volcano at the northern end of the Akaroa Harbour, and radiate out from the geometric centre of the Akaroa volcano cutting the lava shield. The 'Church-type' lavas (cb, cd, ci; 8·1–7·3 Ma; Stipp & Mc Dougall, 1968) were mainly erupted on the southwestern and central northern flanks of the Lyttelton volcano and are thought to mark the transition between the Akaroa Volcanic Group and the youngest Diamond Harbour Volcanic Group. The Diamond Harbour Volcanic Group (7·0–5·8 Ma; Stipp & Mc Dougall, 1968) comprises the Stoddard Basalt (ds) and the Kaioruru Hawaiite (dk). These lavas occur as scattered outcrops on both volcanoes but predominantly along the NE flank of the Lyttelton volcano and above the northward directed flows of the Mount Herbert Volcanic Group. Small eruption centers of the Diamond Harbour Volcanic Group are also present on the northern to northeastern flanks of the Akaroa volcano (Fig. 1).

ANALYTICAL METHODS

Only the freshest parts of the volcanic rocks were selected for analyses. To remove easily soluble material (e.g. dust cover, salt, etc.), the samples were cleaned in deionized water in an ultrasonic bath and dried overnight at 50°C. After sieving the clean grains into several fractions, the samples were carefully hand-picked under a binocular microscope and then reduced to powder in an agate ball mill for major and trace element and isotope analyses.

Major element analyses were carried out on fused glass beads by X-ray fluorescence spectrometry (XRF) on a Phillips X'Unique PW 1480 instrument using a Rh-tube at the Leibniz Institute of Marine Sciences (IFM-GEOMAR). To produce homogeneous glass beads, 0·6 mg of dry sample powder, lithium tetraborate and ammonium nitrate were mixed in platinum cups and then fused in four heat-steps.

Trace element analyses were carried out by quadrupole inductively coupled mass spectrometry (ICP-MS) using an Agilent 7500c/s system at the Institute for Geosciences of the University of Kiel. The samples were prepared following the pressurized mixed acid (aqua regia + $HClO_4$) digestion method, as described by Garbe-Schönberg (1993).

Major element contents in internal rock standards (JB-2, JB-3, JA-1) measured with the samples are generally within 5% of the expected values (Govindaraju, 1994; see Supplementary Data Table 1, available for downloading at http://www.petrology.oxfordjournals.org). H_2O and CO_2 concentrations were determined by means of an IR photometer (Rosemount CSA 5003). Replicate digestions and analyses were used to determine precision. The external precision of the determined trace elements is better than

Table 1: $^{40}Ar/^{39}Ar$ age determinations

Sample	Phase	Unit	Sample locality	Rock type	Plateau age (Ma)	2σ	MSWD	%^{39}Ar plateau
Lyttelton volcano (including Governors Bay Formation and Allandale Rhyolite)								
MSI13	plag	Lyttelton volcano (l)	S43°36′41·5″, E172°40′20·0″	alkali basalt	12·28	±0·73	0·93	90·2
MSI107	plag	Lyttelton volcano (l)	S43°39′39·2″, E172°37′15·2″	alkali basalt	12·11	±0·43	1·11	84·1
MV-4	alkali fsp	Allandale Rhyolite (ra)	S43°41′25·6″, E172°38′18·4″	rhyolite	11·65	±0·03	0·49	$n=12$
MSI114	plag	Governors Bay Formation (gd)	S43°37′59·7″, E172°38′56·9″	benmoreite	11·52	±0·11	0·61	91·3
MSI9A	plag	Lyttelton volcano (lp)	S43°33′24·30″, E172°43′55·20″	mugearite	10·74	±0·32	1·80	80·7
Akaroa volcano (including Mount Herbert and Diamond Harbour Volcanic Groups)								
MSI144	plag	Akaroa volcano (ae)	S43°50′59·0″, E172°58′11·3″	alkali basalt	9·37	±0·42	1·03	82·6
MSI18	plag	Akaroa volcano (af)	S43°45′39·2″, E173°03′22·6″	alkali basalt	9·07	±0·13	0·70	100
MSI117	mx	Mount Herbert Volcanic Group (hh)	S43°41′22·7″, E172°44′30·0″	hawaiite	9·07	±0·20	0·79	80·2
N36C3602	bt	Akaroa volcano (ao)	S43°46′20·46″, E172°55′38·06″	syenite	8·85	±0·08	0·65	62·8
UC13809	mx	Akaroa volcano (af)	S43°43′34·56″, E173°02′55·91″	alkali basalt	8·78	±1·40	1·08	75·2
MSI20E	mx	Diamond Harbour Volcanic Group (ds); LBPI	S43°44′20·8″, E173°04′14·1″	basanite	8·42	±0·16	1·00	86·9
CD103	plag	Mount Herbert Volcanic Group (hh)	S43°41′08·35″, E172°44′26·49″	alkali basalt	8·26	±0·66	1·30	100·0
CD112	plag	Diamond Harbour Volcanic Group (ds)	S43°40′15·61″, E172°44′03·96″	alkali basalt	7·56	±0·52	0·55	87·1
CD77	mx	Diamond Harbour Volcanic Group (ds)	S43°38′10·03″, E172°43′22·52″	transitional tholeiite	7·12	±0·32	1·60	64·8
CD77	mx duplicate	Diamond Harbour Volcanic Group (ds)	S43°38′10·03″, E172°43′22·52″	transitional tholeiite	6·82	±0·36	1·70	83·6

Unit descriptions are after Sewell *et al.*, (1992). fsp, feldspar; plag, plagioclase; mx, matrix; bt, biotite. LBPI, Le Bons Peak intrusion.

6%. Trace element compositions of BHVO-2 and AGV-1 measured along with the samples were within 7% of the US Geological Survey working values, except for Li, Nb, Ta, Lu, Cs (10–17%) and Cr, Sb, Tm (21–26%; see Supplementary Data Table 1).

Sr, Nd, Pb and Hf isotope measurements were conducted at IFM-GEOMAR. For isotope determination, ~200 mg of sample powder was dissolved in a hot HF–HNO_3 mixture followed by the ion exchange procedure of Hoernle *et al.* (2008) to separate Sr, Nd and Pb from the matrix. Sr isotopes were analyzed by thermal ionization mass spectrometry (TIMS) on ThermoFinnigan Triton and Finnigan MAT262 RPQ^{2+} systems operating in static mode; Nd isotope measurements by TIMS on a ThermoFinnigan system running in multidynamic mode; Pb isotopes by TIMS on a Finnigan MAT262 RPQ^{2+} system operating in static mode; and Hf isotopes by multicollector ICP-MS using a VG Axiom system. Sr and Nd isotopic ratios were normalized within run to $^{86}Sr/^{88}Sr = 0{\cdot}1194$ and $^{146}Nd/^{144}Nd = 0{\cdot}7219$, respectively. All stated errors are given as 2σ. The average values of standards are: for NBS 987 $^{87}Sr/^{86}Sr = 0{\cdot}710228 \pm 0{\cdot}000023$ ($n=23$), for La Jolla $^{143}Nd/^{144}Nd = 0{\cdot}511858 \pm 0{\cdot}000013$ ($n=6$) and for an in-house Nd monitor SPEX = $0{\cdot}511724 \pm 0{\cdot}000010$ ($n=20$). Isotope ratios were normalized to 0·71025 for $^{87}Sr/^{86}Sr$ and 0·511850 for $^{143}Nd/^{144}Nd$ for La Jolla and 0·511715 for Nd SPEX. Pb standard NBS 981 ($n=19$) gave $^{208}Pb/^{204}Pb = 36{\cdot}527 \pm 0{\cdot}0022$, $^{207}Pb/^{204}Pb = 15{\cdot}591 \pm 0{\cdot}007$, $^{206}Pb/^{204}Pb = 16{\cdot}900 \pm 0{\cdot}005$; the data were corrected to the values given by Todt *et al.* (1996). Pb chemistry blanks are below 400 pg and can therefore be considered as negligible. Hafnium isotopes were determined on the same rock powders as used for Sr, Nd, and Pb isotope measurements. Hafnium was separated following a slightly modified two-column procedure as described by Blichert-Toft *et al.* (1997). After 2 days of measuring the in-house SPEX Hf monitor to stabilize the signal, standards were determined repeatedly every two or three samples to verify the machine performance. To correct for the instrumental mass bias, $^{176}Hf/^{177}Hf$ was normalized to $^{179}Hf/^{177}Hf = 0{\cdot}7325$.

For O isotope analyses, 2–4 mg pristine olivine grains were carefully hand-picked under a binocular microscope. Analyses were carried out at the University of Oregon's stable isotope lab using CO_2 laser fluorination, BrF_5 as a reagent, followed by conversion to CO_2 gas and analysis on a Finnigan MAT 253 gas source mass spectrometer. San Carlos olivine and garnet standards were measured along with the samples. Day-to-day variability was corrected to standard working values with the variability lying within ±0·1 ‰. Duplicates ($n=6$) deviate less than 0·2‰ from each other.

$^{40}Ar/^{39}Ar$ dating was conducted on K-bearing mineral phases, such as feldspar, biotite, and microcrystalline matrix, by laser step-heating at the geochronology laboratory at IFM-GEOMAR using a 20 W Spectra Physics argon laser and a MAP 216 noble gas mass spectrometer. After hand-picking ~20 mg of 250–500 μm chips for matrix and 250 μm–1 mm sized crystals, the samples were cleaned using deionized water and an ultrasonic disintegrator. Feldspar and amphibole crystals were etched for ~15 and 5–10 min in 5% dilute hydrofluoric acid, respectively. The clean samples were loaded in aluminum trays, wrapped in cadmium foil and neutron irradiated at the 5 MW reactor of the GKSS Reactor Centre in Geesthacht, Germany. Raw mass spectrometer peaks were corrected for mass discrimination and background noise, and blanks were measured every fifth analysis. To monitor the neutron flux, the TCR-1 (Taylor Creek Rhyolite, 27·92 Ma; Duffield & Dalrymple, 1990) sanidine standard and an internal standard SAN6165 (0·47 Ma; van den Bogaard, 1995) were used. High purity KSO_4 and CaF_2 salt crystals, analysed at the same time as the samples, were used to correct for Ca and K interferences.

Single fusion analyses were carried out on 0·1–2·5 mg of crystals or matrix chips. To conduct step-heat analyses, 3·8–7·7 mg of sample material (phenocrysts or matrix) were used. Incrementally increasing laser output from 20 mW to 20 W allows continuous determination of the $^{40}Ar/^{39}Ar$ isotope ratio. An age is derived from the plateau proportion of the measured age spectra. All errors are given as 2σ.

RESULTS

Age determinations

New $^{40}Ar/^{39}Ar$ ages for 14 volcanic rocks from the Banks Peninsula volcanoes are presented in Table 1 with errors stated as 2σ (see Supplementary Data Table 1 for more details). Three samples from the Lyttelton volcano yield an age range from 12·3 to 10·7 Ma. The ages from the undifferentiated Lyttelton Volcanic Group (following the classification of Sewell *et al.*, 1992) are 12·28 ± 0·72 and 12·11 ± 0·43 Ma, whereas the stratigraphically younger Mount Pleasant Formation gave an age of 10·74 ± 0·32 Ma. Samples from the Allandale Rhyolite and Governors Bay Formation gave ages of 11·65 ± 0·03 and 11·52 ± 0·11 Ma, respectively, and therefore are within 2σ errors of the basaltic volcanism of the Lyttelton Group. Previous Rb/Sr and K/Ar age dating produced similar ages for the Lyttelton shield (11·9 ± 0·4 to 11·1 ± 0·3 Ma) but younger ages for the Governors Bay Formation and Allandale Rhyolite (10·8 ± 0·1 Ma; Barley & Weaver, 1988, Stipp & Mc Dougall, 1968; Barley *et al.*, 1988).

The Mount Herbert Volcanic Group samples gave $^{40}Ar/^{39}Ar$ ages of 9·07 ± 0·20 and 8·26 ± 0·66 Ma, increasing and extending the K/Ar range (8·5–8 Ma; Stipp & Mc Dougall, 1968) to an older age. Our ages confirm that the Mount Herbert lavas were erupted after the formation of the Lyttelton volcano, but overlap the age range of the Akaroa volcano, for which $^{40}Ar/^{39}Ar$ ages of 9·37 ± 0·42, 9·07 ± 0·13, 8·85 ± 0·08 and 8·78 ± 1·4 Ma are almost identical within 2σ errors. An age of 8·85 ± 0·08 Ma was obtained on biotite from a syenite intrusion on the Onawne Peninsula; this is significantly younger than the former age of 11·8 Ma determined by the K/Ar technique (Stipp & Mc Dougall, 1968). The new $^{40}Ar/^{39}Ar$ age places its formation within the age range of the Akaroa shield lavas. Two samples from the Diamond Harbour Volcanic Group gave ages of 7·56 ± 0·52 and 6·97 ± 0·34 Ma (average of two determinations). One sample from the Le Bons Peak basanite intrusion (Sewell *et al.*, 1992) on the western flank of Akaroa volcano yielded an age of 8·42 ± 0·16 Ma, which is significantly older than the other analyzed samples of the Diamond Harbour Volcanic Group, but identical within error with the age determined on the younger Mount Herbert Group basalt.

In conclusion, the new $^{40}Ar/^{39}Ar$ ages give a revised picture of the temporal evolution of Miocene volcanism on the Banks Peninsula, with both the Lyttelton volcano and Akaroa volcano being slightly older than previously believed. The Mount Herbert Volcanic Group lavas and the Le Bons Peak intrusion were emplaced contemporaneously with the activity at Akaroa volcano.

Sample descriptions and geochemistry

The majority of the 41 moderately mafic (>4 wt %) volcanic rocks from Banks Peninsula are dense, hypo- to holocrystalline and porphyric, containing predominantly olivine, clinopyroxene and plagioclase phenocrysts and Fe–Ti oxide microphenocrysts. Dominant groundmass minerals are plagioclase, clinopyroxene and Fe–Ti oxides. Most of the lavas are fresh, but some show minor secondary alteration. Large kaersutite phenocrysts are present in the late-stage volcanic rocks from Lyttelton volcano (MSI 9A) and as rare, small phenocrysts in the youngest lavas from the Diamond Harbour Volcanic Group (e.g. MSI 128B).

New major element, trace element and Sr, Nd, Pb, Hf and O isotope data are presented in Tables 2 and 3. Lyttelton volcanic rocks (including Governors Bay Formation and Allandale Rhyolite) range from transitional tholeiites to alkali basalts to rhyolites, whereas lavas from Akaroa volcano are generally more undersaturated in silica and fractionate along a trend from picrite to basanite/alkali basalt to trachyte. Mount Herbert lavas have similar compositions to the Akaroa lavas, ranging from alkali basalt to tephrite. The similarity in age and geochemistry suggests that the Mount Herbert lavas are

Table 2: Major and trace element compositions

Sample:	MSI 9A	MSI 10	MSI 12B	MSI 13	MSI 15	MSI 100A	MSI 102
Latitude (S):	43°33′24·3″	43°35′44·0″	43°36′22·5″	43°36′41·5″	43°38′57·5″	43°36′02·6″	43°34′54·0″
Longitude (E):	172°43′55·2″	172°44′53·2″	172°41′25·4″	172°40′20·0″	172°39′30·4″	172°44′26·5″	172°43′31·2″
Unit:	lp	l	gd	l	ra	l	l
Lyttleton Group							
Major elements (wt %; determined by XRF)							
SiO_2	49·87	48·65	55·45	50·39	74·99	61·26	52·23
TiO_2	2·20	2·83	3·44	3·66	0·04	1·28	2·00
Al_2O_3	16·07	16·67	18·24	15·32	13·44	15·55	17·52
FeO^t	10·30	10·99	4·78	12·42	0·75	7·35	9·48
MnO	0·14	0·17	0·05	0·14	0·02	0·11	0·17
MgO	5·05	4·54	1·54	3·39	0·09	1·65	2·74
CaO	7·14	8·76	6·46	7·85	0·09	4·02	6·30
Na_2O	4·89	3·83	5·20	3·37	3·60	4·26	5·41
K_2O	2·05	1·28	1·97	1·30	4·48	3·34	2·32
P_2O_5	0·60	0·62	1·00	0·58	0·01	0·34	0·77
CO_2	0·01	0·10	0·03	0·04	0·01	0·07	0·02
H_2O	0·71	1·45	1·25	1·24	1·09	1·13	0·61
Total	99·03	99·89	99·41	99·70	98·61	100·36	99·57
Trace elements (ppm; determined by ICP-MS)							
Li	11·2	8·88	n.a.	7·03	175	n.a.	n.a.
Sc	14·6	18·6	n.a.	24·7	0·50	n.a.	n.a.
V	163	187	n.a.	307	2·20	n.a.	n.a.
Cr	129	52·9	n.a.	15·1	1·16	n.a.	n.a.
Co	38·8	33·0	n.a.	33·3	0·91	n.a.	n.a.
Ni	101	39·7	n.a.	24·8	0·65	n.a.	n.a.
Cu	48·9	44·0	n.a.	35·7	3·43	n.a.	n.a.
Zn	154	129	n.a.	154	84·8	n.a.	n.a.
Ga	27·4	24·3	n.a.	25·9	54·2	n.a.	n.a.
Rb	52·9	28·4	n.a.	37·3	694	n.a.	n.a.
Sr	723.	565	n.a.	482	5·11	n.a.	n.a.
Y	27·7	33·2	n.a.	39·1	41·2	n.a.	n.a.
Zr	358	245.	n.a.	272	62·8	n.a.	n.a.
Nb	72·8	50·5	n.a.	48·4	108	n.a.	n.a.
Mo	3·93	2·30	n.a.	2·21	0·38	n.a.	n.a.
Cd	n.a.	n.a.	n.a.	n.a.	n.a.	n.a.	n.a.
Sn	3·02	2·32	n.a.	2·26	36·9	n.a.	n.a.
Sb	0·12	0·06	n.a.	0·06	0·77	n.a.	n.a.
Cs	1·14	0·44	n.a.	0·67	8·56	n.a.	n.a.
Ba	532	309	n.a.	361	22·4	n.a.	n.a.
La	54·5	36·3	n.a.	39·9	13·9	n.a.	n.a.
Ce	102	73·9	n.a.	75·7	31·8	n.a.	n.a.
Pr	12·6	9·53	n.a.	10·8	4·77	n.a.	n.a.
Nd	47·7	38·7	n.a.	44·5	18·9	n.a.	n.a.
Sm	9·36	8·41	n.a.	9·83	6·25	n.a.	n.a.
Eu	3·02	2·77	n.a.	3·06	0·10	n.a.	n.a.
Gd	8·46	8·15	n.a.	9·67	7·02	n.a.	n.a.
Tb	1·17	1·21	n.a.	1·43	1·48	n.a.	n.a.
Dy	5·98	6·63	n.a.	7·88	10·4	n.a.	n.a.
Ho	1·03	1·23	n.a.	1·45	2·26	n.a.	n.a.
Er	2·30	3·02	n.a.	3·54	6·89	n.a.	n.a.
Tm	0·32	0·41	n.a.	0·49	1·19	n.a.	n.a.
Yb	1·89	2·51	n.a.	2·95	8·03	n.a.	n.a.
Lu	0·26	0·36	n.a.	0·42	1·05	n.a.	n.a.
Hf	7·97	5·76	n.a.	6·68	4·63	n.a.	n.a.
Ta	4·35	2·87	n.a.	2·78	21·4	n.a.	n.a.
W	1·41	0·45	n.a.	0·89	13·9	n.a.	n.a.
Tl	0·06	0·02	n.a.	0·03	3·11	n.a.	n.a.
Pb	4·80	3·09	n.a.	4·83	14·4	n.a.	n.a.
Th	8·32	4·23	n.a.	5·50	40·9	n.a.	n.a.
U	2·19	1·06	n.a.	1·37	8·81	n.a.	n.a.

(continued)

Table 2: Continued

Sample:	MSI 103	MSI 105	MSI 107	MSI 108	MSI 112	MSI 113	MSI 114
Latitude (S):	43°35′42·9″	43°37′47·4″	43°39′39·2″	43°41′17·9″	43°41′26·6″	43°40′08·5″	43°37′59·7″
Longitude (E):	172°39′58·5″	172°37′31·6″	172°37′15·2″	172°38′29·8″	172°38′17·2″	172°37′31·4″	172°38′56·9″
Unit:	l	l	l	t	ra	l	gd
Lyttleton Group							
Major elements (wt %; determined by XRF)							
SiO_2	48·76	69·83	47·86	77·85	77·04	47·26	60·10
TiO_2	3·32	0·22	2·69	0·08	0·08	2·94	1·43
Al_2O_3	14·49	13·51	17·49	11·89	11·62	15·80	14·24
FeO^t	12·51	3·34	10·55	0·96	1·65	12·17	6·59
MnO	0·16	0·07	0·15	0·01	0·01	0·15	0·09
MgO	3·76	0·03	4·88	0·12	0·18	4·69	2·95
CaO	7·73	0·32	9·17	0·29	0·27	9·10	4·39
Na_2O	3·86	5·81	3·51	3·26	2·87	3·40	3·84
K_2O	1·50	4·91	1·14	4·60	4·34	1·17	3·40
P_2O_5	0·65	0·05	0·58	0·01	0·02	0·59	0·29
CO_2	0·11	0·02	0·08	0·02	0·05	0·58	1·11
H_2O	1·82	0·50	1·18	0·69	1·06	1·56	0·97
Total	98·67	98·61	99·28	99·78	99·19	99·41	99·40
Trace elements (ppm; determined by ICP-MS)							
Li	6·00	50·5	7·85	49·2	n.a.	6·32	14·2
Sc	22·2	0·61	18·2	1·24	n.a.	19·4	12·2
V	215	3·13	211	2·42	n.a.	231	116
Cr	1·55	1·04	93·6	0·85	n.a.	85·6	77·0
Co	35·1	0·04	34·9	0·41	n.a.	44·8	21·9
Ni	3·01	0·59	57·6	0·63	n.a.	88·6	42·3
Cu	17·3	5·79	42·9	1·60	n.a.	50·1	17·6
Zn	160	175	108	58·8	n.a.	124	101
Ga	25·9	36·5	23·8	29·3	n.a.	23·2	25·2
Rb	34·0	202	29·6	321	n.a.	29·1	116
Sr	489	5·06	635	11·0	n.a.	541	288
Y	39·0	73·3	24·0	41·7	n.a.	27·8	36·8
Zr	275	953	234	141	n.a.	239	204
Nb	54·9	134	42·4	61·3	n.a.	44·7	42·2
Mo	2·42	1·15	n.a.	0·72	n.a.	n.a.	3·03
Cd	n.a.	n.a.	n.a.	0·40	n.a.	n.a.	n.a.
Sn	2·57	9·91	1·96	11·1	n.a.	2·07	3·87
Sb	0·07	0·41	0·03	0·97	n.a.	0·07	0·31
Cs	0·39	0·76	0·98	9·71	n.a.	0·55	3·44
Ba	331	17·1	262	25·1	n.a.	274	462
La	39·8	101	32·1	31·3	n.a.	32·6	50·8
Ce	82·2	138	66·6	65·0	n.a.	67·9	99·3
Pr	10·7	23·4	8·27	7·95	n.a.	8·52	12·2
Nd	43·9	83·6	33·7	28·1	n.a.	35·0	45·6
Sm	9·74	16·6	7·30	7·12	n.a.	7·68	9·33
Eu	3·16	0·78	2·45	0·18	n.a.	2·49	1·73
Gd	9·71	15·3	7·07	6·72	n.a.	7·48	8·62
Tb	1·44	2·45	1·02	1·24	n.a.	1·09	1·31
Dy	7·98	14·2	5·58	7·79	n.a.	5·99	7·22
Ho	1·48	2·75	1·00	1·55	n.a.	1·08	1·34
Er	3·66	7·27	2·46	4·40	n.a.	2·65	3·38
Tm	0·50	1·09	0·33	0·69	n.a.	0·35	0·47
Yb	3·08	7·00	1·99	4·51	n.a.	2·16	2·94
Lu	0·43	1·01	0·27	0·61	n.a.	0·30	0·41
Hf	6·85	24·3	5·20	6·78	n.a.	5·37	6·01
Ta	3·33	8·32	2·59	5·33	n.a.	2·73	2·70
W	0·69	2·46	0·60	n.a.	n.a.	1·02	2·39
Tl	0·03	0·52	0·03	1·39	n.a.	0·03	0·34
Pb	2·97	17·3	3·33	28·1	n.a.	3·11	12·6
Th	5·28	30·2	3·93	39·2	n.a.	4·18	13·4
U	1·34	2·44	1·04	8·53	n.a.	0·98	3·01

(continued)

Table 2: Continued

Sample:	MSI 125A	MSI 126	MSI 130	MSI 131B	CD103	M36B 2259	N36C 3069
Latitude (S):	43°33′24·3″	43°35′44·0″	43°36′22·5″	43°36′41·5″	43°41′08·4″	43°41′41·0″	43°46′23·0″
Longitude (E):	172°43′55·2″	172°44′53·2″	172°41′25·4″	172°40′20·0″	172°44′26·5″	172°44′26·5″	172°54′46·5″
Unit:	l	ec	l	l	hh	ho	af
Lyttleton and Akaroa Group							
Major elements (wt %; determined by XRF)							
SiO_2	49·08	92·79	60·29	49·35	45·70	44·74	47·30
TiO_2	1·99	0·11	1·40	2·96	3·36	3·13	2·86
Al_2O_3	14·54	2·59	15·61	14·59	15·84	14·12	16·86
FeO^t	10·64	0·14	7·47	12·87	13·00	12·92	11·82
MnO	0·15	0·00	0·12	0·18	0·18	0·16	0·20
MgO	8·50	0·12	1·56	4·27	6·23	9·13	4·09
CaO	9·29	0·05	4·28	8·05	8·92	10·30	7·49
Na_2O	3·26	<0·01	4·15	3·90	3·50	2·28	4·49
K_2O	1·08	0·67	3·30	1·36	1·19	0·87	1·69
P_2O_5	0·46	0·01	0·39	0·70	0·58	0·42	0·82
CO_2	0·11	0·00	0·21	0·06	0·54	0·70	1·30
H_2O	0·89	0·64	0·96	1·35	0·01	1·70	0·08
Total	99·99	97·12	99·74	99·64	99·05	100·47	99·00
Trace elements (ppm; determined by ICP-MS)							
Li	8·49	5·65	23·4	6·67	8·98	7·97	11·0
Sc	20·4	1·44	11·5	22·8	27·3	38·9	17·6
V	198	21·4	93·6	234	305	424	150
Cr	248	16·7	7·55	60·3	141	407	2·37
Co	44·7	0·17	15·8	37·0	56·1	78·6	36·5
Ni	179	0·46	12·1	33·7	88·1	232	4·01
Cu	54·7	0·49	17·3	41·6	60·0	103	28·5
Zn	99·5	2·04	114	177	150	141	163
Ga	19·1	2·82	26·1	26·0	n.a.	n.a.	n.a.
Rb	25·8	34·2	113	31·9	28·6	26·2	45·1
Sr	512	3·75	374	493	796	688	963
Y	21·5	1·99	41·1	37·7	31·6	25·2	38·7
Zr	157	5·61	411	247·6	221	176	312
Nb	36·5	1·56	44·6	50·2	54·4	41·7	78·8
Mo	1·56	0·06	2·78	2·51	n.a.	n.a.	n.a.
Cd	0·13	0·02	0·26	n.a.	n.a.	n.a.	n.a.
Sn	1·61	0·37	4·50	2·23	1·72	1·43	2·06
Sb	0·08	0·11	0·20	0·09	0·06	0·05	0·09
Cs	0·35	3·56	4·28	0·48	0·29	0·29	0·46
Ba	306	56·9	705	334·7	322	242	427
La	26·5	2·76	57·2	38·6	31·3	24·5	46·2
Ce	54·2	7·21	118	79·4	64·5	50·3	94·1
Pr	6·75	0·68	13·9	10·4	7·82	6·02	11·1
Nd	27·8	2·45	53·5	42·7	31·9	24·4	43·6
Sm	6·02	0·48	10·8	9·46	7·02	5·44	9·07
Eu	1·99	0·07	2·56	3·07	2·30	1·78	2·85
Gd	5·91	0·41	10·2	9·37	6·33	4·92	7·80
Tb	0·85	0·06	1·50	1·38	0·98	0·76	1·18
Dy	4·56	0·35	8·18	7·63	5·26	4·12	6·26
Ho	0·82	0·07	1·52	1·41	0·94	0·73	1·12
Er	2·01	0·20	3·97	3·44	2·38	1·83	2·84
Tm	0·27	0·03	0·55	0·47	0·31	0·23	0·36
Yb	1·63	0·21	3·53	2·85	1·89	1·45	2·26
Lu	0·23	0·03	0·50	0·40	0·26	0·20	0·31
Hf	3·76	0·22	10·3	6·20	4·27	3·37	5·46
Ta	2·09	0·12	2·70	2·93	2·70	1·98	3·66
W	n.a.	n.a.	n.a.	0·88	n.a.	n.a.	n.a.
Tl	0·04	0·08	0·54	0·03	n.a.	n.a.	n.a.
Pb	3·69	0·61	16·9	5·16	2·20	1·61	3·14
Th	3·95	1·13	14·5	5·02	3·66	3·14	5·57
U	0·98	0·19	3·59	1·27	0·93	0·78	1·38

(continued)

Table 2: Continued

Sample:	N36C 3072	N36C 3602	UC 13809	MSI 18	MSI 117	MSI 120	MSI 123
Latitude (S):	43°47′45·8′	43°46′20·46″	43°43′34·56″	43°45′39·2″	43°41′22·7″	43°41′42·1″	43°41′00·4″
Longitude (E):	172°54′29·9″	172°55′38·06″	173°02′55·91″	173°03′22·6″	172°44′30·0″	172°43′24·6″	172°43′24·6″
Unit:	af	ao	af	af	hh	ho	ho
Akaroa Group							
Major elements (wt %; determined by XRF)							
SiO_2	43·67	42·09	44·52	45·12	47·71	45·07	46·72
TiO_2	2·85	4·11	3·57	3·50	2·65	3·73	2·58
Al_2O_3	13·01	15·27	15·98	15·99	17·28	15·36	17·10
FeO^t	13·22	13·31	12·90	12·91	11·66	13·34	12·03
MnO	0·18	0·16	0·17	0·18	0·19	0·17	0·21
MgO	10·28	5·02	6·24	6·39	3·91	6·95	3·97
CaO	10·56	11·62	10·40	9·63	7·69	9·72	8·07
Na_2O	2·35	2·66	2·85	3·25	4·99	3·20	4·02
K_2O	0·96	0·36	1·01	1·11	1·69	0·85	1·79
P_2O_5	0·39	0·23	0·50	0·59	0·98	0·46	1·45
CO_2	1·94	0·87	0·04	0·08	0·02	0·05	0·06
H_2O	0·06	3·45	1·43	1·54	0·59	0·83	1·90
Total	99·47	99·15	99·61	100·29	99·36	99·73	99·90
Trace elements (ppm; determined by ICP-MS)							
Li	7·26	5·54	5·92	5·24	8·21	3·95	5·68
Sc	42·1	49·0	33·2	21·8	9·60	24·1	9·42
V	468	583	430	271	112	318	108
Cr	497	2·47	177	117	1·59	173	3·29
Co	87·4	61·2	62·9	47·4	29·6	56·2	31·5
Ni	263	20·4	82·5	61·1	8·60	114	8·78
Cu	87·0	64·8	58·5	53·3	32·2	79·0	30·4
Zn	144	142	154	126	135	132	152
Ga	n.a.	n.a.	n.a.	22·2	23·3	22·6	25·3
Rb	32·7	9·38	30·7	23·2	37·5	17·2	42·1
Sr	548	614	801	726	901	676	1052
Y	25·0	16·3	27·5	28·0	33·7	25·9	36·7
Zr	167	79·6	206·7	208	283	194	361
Nb	38·0	22·8	50·1	52·4	75·7	43·1	83·7
Mo	n.a.	n.a.	n.a.	2·14	3·01	1·91	4·14
Cd	n.a.	n.a.	n.a.	n.a.	n.a.	n.a.	n.a.
Sn	1·44	0·90	1·61	1·75	2·11	1·70	2·01
Sb	0·05	0·03	0·05	0·06	0·09	0·04	0·11
Cs	0·26	0·29	0·24	0·24	0·42	0·27	0·47
Ba	217	113	268	313	457	271	484
La	22·2	9·98	28·3	32·3	48·8	27·2	64·5
Ce	46·6	21·7	58·0	66·4	98·4	56·1	129
Pr	5·62	2·80	6·92	8·61	12·4	7·24	16·1
Nd	23·2	12·4	28·0	35·3	48·8	29·9	62·5
Sm	5·27	3·09	6·17	7·66	9·78	6·64	12·0
Eu	1·71	1·29	2·03	2·57	3·13	2·28	3·76
Gd	4·83	3·05	5·52	7·39	8·96	6·58	10·6
Tb	0·75	0·49	0·85	1·07	1·26	0·96	1·46
Dy	4·10	2·70	4·53	5·79	6·71	5·28	7·59
Ho	0·74	0·48	0·80	1·06	1·22	0·96	1·35
Er	1·82	1·20	1·98	2·49	2·95	2·34	3·27
Tm	0·23	0·16	0·26	0·34	0·40	0·32	0·43
Yb	1·41	0·94	1·53	2·07	2·45	1·88	2·59
Lu	0·19	0·13	0·21	0·29	0·34	0·27	0·37
Hf	3·28	1·73	3·87	4·89	6·05	4·61	7·70
Ta	1·81	1·16	2·39	3·08	4·19	2·53	4·42
W	n.a.	n.a.	n.a.	0·68	0·70	0·42	1·18
Tl	n.a.	n.a.	n.a.	0·03	0·03	0·03	0·06
Pb	1·91	0·82	1·72	1·99	2·94	1·65	3·44
Th	2·74	0·98	3·48	3·63	5·58	3·24	7·30
U	0·71	0·23	0·88	0·96	1·49	0·89	1·98

(continued)

Table 2: Continued

Sample:	MSI 134	MSI 137	MSI 141	MSI 144	MSI 148	MSI 150	MSI 151
Latitude (S):	43°40′21·3″	43°40′50·2″	43°49′30·0″	43°50′59·0″	43°40′08·0″	43°43′02·4″	43°41′46·9″
Longitude (E):	172°49′57·7″	172°51′12·1″	172°56′49·7″	172°58′11·3″	172°59′40·5″	172°58′23·8″	173°03′53·7″
Unit:	hp	hp	af	ae	af	af	af
Akaroa Group							
Major elements (wt %; determined by XRF)							
SiO_2	44·37	46·63	45·92	44·93	47·09	45·29	49·24
TiO_2	3·66	2·98	3·28	3·59	3·09	3·59	2·25
Al_2O_3	16·03	16·72	16·34	16·01	17·10	16·09	17·28
FeO^t	13·18	12·36	11·42	12·90	11·73	13·15	10·91
MnO	0·17	0·19	0·15	0·18	0·18	0·17	0·21
MgO	5·54	4·55	5·02	4·94	4·62	6·24	2·90
CaO	8·94	7·61	8·99	8·71	8·12	10·00	7·08
Na_2O	3·46	4·12	3·22	3·34	4·15	2·89	5·21
K_2O	1·15	1·49	1·21	1·27	1·57	0·98	2·02
P_2O_5	0·51	0·76	0·60	0·61	0·85	0·49	1·14
CO_2	0·09	0·02	1·15	0·05	0·05	0·07	0·21
H_2O	1·85	1·30	1·61	1·47	1·66	1·12	0·58
Total	98·95	98·73	98·91	98·00	100·21	100·08	99·03
Trace elements (ppm; determined by ICP-MS)							
Li	5·82	6·15	n.a.	5·77	6·69	n.a.	n.a.
Sc	17·5	13·2	n.a.	17·5	12·5	n.a.	n.a.
V	260	143	n.a.	214	157	n.a.	n.a.
Cr	31·8	16·0	n.a.	27·0	12·3	n.a.	n.a.
Co	48·3	34·7	n.a.	38·7	31·3	n.a.	n.a.
Ni	37·5	13·0	n.a.	21·1	11·9	n.a.	n.a.
Cu	41·2	32·9	n.a.	24·3	23·5	n.a.	n.a.
Zn	136	136	n.a.	138	141	n.a.	n.a.
Ga	23·7	23·3	n.a.	22·3	24·1	n.a.	n.a.
Rb	29·8	32·7	n.a.	27·5	33·2	n.a.	n.a.
Sr	741	807	n.a.	1080	835	n.a.	n.a.
Y	26·0	32·0	n.a.	31·6	33·3	n.a.	n.a.
Zr	202	270	n.a.	246	304	n.a.	n.a.
Nb	49·2	65·5	n.a.	56·6	73·4	n.a.	n.a.
Mo	2·06	2·68	n.a.	2·26	3·15	n.a.	n.a.
Cd	n.a.	n.a.	n.a.	n.a.	n.a.	n.a.	n.a.
Sn	1·87	2·25	n.a.	1·99	2·36	n.a.	n.a.
Sb	0·05	0·07	n.a.	0·04	0·07	n.a.	n.a.
Cs	0·75	0·29	n.a.	0·16	0·28	n.a.	n.a.
Ba	311	388	n.a.	348	409	n.a.	n.a.
La	31·9	43·4	n.a.	36·2	47·3	n.a.	n.a.
Ce	64·1	87·0	n.a.	72·7	94·2	n.a.	n.a.
Pr	8·17	11·0	n.a.	9·47	11·9	n.a.	n.a.
Nd	33·4	43·9	n.a.	38·5	47·2	n.a.	n.a.
Sm	7·17	9·08	n.a.	8·36	9·68	n.a.	n.a.
Eu	2·43	3·00	n.a.	2·78	3·15	n.a.	n.a.
Gd	6·91	8·47	n.a.	8·04	8·97	n.a.	n.a.
Tb	1·00	1·21	n.a.	1·16	1·27	n.a.	n.a.
Dy	5·38	6·52	n.a.	6·26	6·70	n.a.	n.a.
Ho	0·97	1·20	n.a.	1·14	1·20	n.a.	n.a.
Er	2·31	2·92	n.a.	2·77	2·90	n.a.	n.a.
Tm	0·31	0·40	n.a.	0·37	0·39	n.a.	n.a.
Yb	1·84	2·42	n.a.	2·21	2·32	n.a.	n.a.
Lu	0·26	0·35	n.a.	0·31	0·33	n.a.	n.a.
Hf	4·82	6·37	n.a.	5·61	6·58	n.a.	n.a.
Ta	2·85	3·88	n.a.	3·20	4·09	n.a.	n.a.
W	0·52	0·56	n.a.	0·40	0·66	n.a.	n.a.
Tl	0·02	0·02	n.a.	0·02	0·03	n.a.	n.a.
Pb	2·47	2·86	n.a.	2·01	2·88	n.a.	n.a.
Th	4·10	5·08	n.a.	4·05	5·67	n.a.	n.a.
U	1·07	1·34	n.a.	1·01	1·53	n.a.	n.a.

(continued)

Table 2: Continued

Sample:	MSI 154	MSI 157	MSI 161	MSI 164	MSI 167B	MSI 169	MSI 171
Latitude (S):	43°44′21·9″	43°48′03·2″	43°47′33·8″	43°45′10·7″	43°47′39·7″	43°50′51·7″	43°50′19·4″
Longitude (E):	173°05′26·7″	173°00′21·1″	173°01′15·5″	172°52′23·6″	172°54′31·0″	172°53′42·3″	172°52′14·5″
Unit:	af	ae	af	af	af	af	ae
Akaroa Group							
Major elements (wt %; determined by XRF)							
SiO_2	47·14	50·44	46·26	45·90	58·81	46·14	46·45
TiO_2	3·08	2·20	3·78	3·36	0·65	3·60	3·62
Al_2O_3	17·26	16·78	15·96	16·28	17·41	16·74	16·48
FeO^t	11·70	10·81	12·87	11·41	5·59	12·88	13·05
MnO	0·18	0·24	0·20	0·17	0·15	0·19	0·19
MgO	4·30	3·09	4·73	4·41	0·60	4·86	4·74
CaO	8·07	6·63	9·13	8·80	1·74	8·57	8·79
Na_2O	4·40	5·08	3·80	3·51	6·25	4·07	3·57
K_2O	1·55	2·09	1·27	1·33	4·32	1·27	1·29
P_2O_5	0·92	1·04	0·69	0·66	0·20	0·70	0·67
CO_2	0·07	0·04	0·52	2·10	2·22	0·09	0·68
H_2O	1·45	0·71	1·21	1·60	0·73	0·69	1·12
Total	100·12	99·15	100·42	99·53	98·67	99·80	100·65
Trace elements (ppm; determined by ICP-MS)							
Li	6·54	n.a.	5·60	6·66	11·5	n.a.	n.a.
Sc	12·1	n.a.	17·1	18·1	3·60	n.a.	n.a.
V	142	n.a.	231	212	2·71	n.a.	n.a.
Cr	2·85	n.a.	4·37	37·4	0·94	n.a.	n.a.
Co	30·7	n.a.	38·5	37·6	2·81	n.a.	n.a.
Ni	5·12	n.a.	9·19	24·6	0·83	n.a.	n.a.
Cu	27·7	n.a.	19·7	34·0	9·34	n.a.	n.a.
Zn	139	n.a.	140	134	150·6	n.a.	n.a.
Ga	24·0	n.a.	23·5	23·2	28·7	n.a.	n.a.
Rb	33·5	n.a.	25·6	31·1	71·7	n.a.	n.a.
Sr	846	n.a.	748	767	207	n.a.	n.a.
Y	34·8	n.a.	32·4	32·1	36·6	n.a.	n.a.
Zr	284	n.a.	243	244	591	n.a.	n.a.
Nb	72·3	n.a.	57·8	58·5	103	n.a.	n.a.
Mo	3·12	n.a.	2·09	1·99	2·73	n.a.	n.a.
Cd	n.a.	n.a.	n.a.	n.a.	n.a.	n.a.	n.a.
Sn	1·92	n.a.	2·02	2·02	5·20	n.a.	n.a.
Sb	0·07	n.a.	0·08	0·04	0·49	n.a.	n.a.
Cs	0·33	n.a.	0·23	0·39	0·77	n.a.	n.a.
Ba	434	n.a.	336	365	1100	n.a.	n.a.
La	47·4	n.a.	36·2	38·0	56·4	n.a.	n.a.
Ce	94·7	n.a.	73·9	78·1	106	n.a.	n.a.
Pr	12·0	n.a.	9·56	10·1	12·6	n.a.	n.a.
Nd	48·0	n.a.	39·2	41·1	44·6	n.a.	n.a.
Sm	9·82	n.a.	8·54	8·81	8·55	n.a.	n.a.
Eu	3·20	n.a.	2·83	2·92	2·50	n.a.	n.a.
Gd	9·19	n.a.	8·27	8·51	7·59	n.a.	n.a.
Tb	1·30	n.a.	1·20	1·23	1·17	n.a.	n.a.
Dy	6·94	n.a.	6·49	6·66	6·69	n.a.	n.a.
Ho	1·26	n.a.	1·18	1·22	1·30	n.a.	n.a.
Er	3·03	n.a.	2·84	2·94	3·51	n.a.	n.a.
Tm	0·41	n.a.	0·38	0·40	0·53	n.a.	n.a.
Yb	2·49	n.a.	2·31	2·40	3·50	n.a.	n.a.
Lu	0·35	n.a.	0·33	0·34	0·51	n.a.	n.a.
Hf	6·23	n.a.	5·55	5·90	12·7	n.a.	n.a.
Ta	3·90	n.a.	3·28	3·44	6·03	n.a.	n.a.
W	0·86	n.a.	0·35	0·39	1·38	n.a.	n.a.
Tl	0·08	n.a.	0·04	0·03	0·14	n.a.	n.a.
Pb	2·68	n.a.	2·16	2·46	9·44	n.a.	n.a.
Th	5·38	n.a.	4·14	4·45	13·9	n.a.	n.a.
U	1·41	n.a.	1·27	1·16	2·02	n.a.	n.a.

(continued)

Table 2: Continued

Sample:	MSI 174	MSI 177	MSI 179	CD77	CD112	UC13790	MSI 16
Latitude (S):	43°48′22·0″	43°49′33·9″	43°45′37·9″	43°38′10·03″	43°40′15·61″	43°43′34·56″	43°37′50·2″
Longitude (E):	172°47′30·4″	172°42′52·9″	172°43′33·7″	172°43′22·52″	172°44′03·96″	173°02′55·91″	172°44′35·9″
Unit:	af	af	ho	sb	sb	sb; LBPI	sb
Akaroa and Diamond Harbour Volcanic Groups							
Major elements (wt %; determined by XRF)							
SiO_2	44·77	45·95	46·49	48·06	45·53	41·86	49·38
TiO_2	3·50	2·94	3·15	1·94	3·22	2·79	1·87
Al_2O_3	16·35	16·24	16·62	13·82	15·81	12·13	14·43
FeOt	12·60	12·43	12·10	11·34	12·89	12·94	11·10
MnO	0·17	0·18	0·17	0·15	0·18	0·18	0·16
MgO	5·85	6·15	4·93	9·24	6·32	11·99	8·79
CaO	9·95	9·49	7·96	9·24	9·50	10·66	9·27
Na_2O	3·17	3·83	4·17	2·95	3·53	2·95	3·14
K_2O	1·14	1·11	1·45	1·03	1·27	1·21	1·05
P_2O_5	0·67	0·77	0·76	0·39	0·60	0·69	0·39
CO_2	0·14	0·04	0·07	0·59	0·56	0·07	0·01
H_2O	1·80	0·75	1·24	0·05	0·04	2·06	0·47
Total	100·11	99·88	99·11	98·80	99·45	99·53	99·99
Trace elements (ppm; determined by ICP-MS)							
Li	5·36	5·31	6·00	13·2	8·73	10·4	8·47
Sc	21·5	20·3	15·8	33·3	29·7	32·4	22·6
V	276	229	193	295	348	380	203
Cr	56·1	152	33·6	457	155	660	302
Co	46·7	48·1	38·4	67·1	58·4	87·5	48·7
Ni	52·2	79·3	25·5	302	95·5	426	213
Cu	60·6	60·5	41·7	84·4	63·6	97·8	80·8
Zn	129	137	141	129	149	169	107
Ga	23·1	23·8	25·8	n.a.	n.a.	n.a.	19·1
Rb	24·0	25·9	32·3	30·9	32·5	52·3	27·0
Sr	810	779	984	494	776	860	440
Y	28·9	28·8	31·7	23·7	30·5	25·2	24·1
Zr	230	215	283	138·8	242	235	149
Nb	57·8	55·7	65·4	33·6	58·3	73·5	33·8
Mo	2·40	2·57	2·83	n.a.	n.a.	n.a.	1·48
Cd	n.a.	n.a.	n.a.	n.a.	n.a.	n.a.	0·11
Sn	2·06	1·72	2·42	1·33	1·86	1·74	1·26
Sb	0·04	0·06	0·07	0·08	0·07	0·08	0·07
Cs	0·22	0·31	0·31	0·59	0·30	0·31	0·51
Ba	342	342	412	257	324	389	288
La	37·1	37·6	44·4	20·9	34·7	44·3	24·7
Ce	75·4	75·8	88·5	43·5	70·0	88·6	47·5
Pr	9·66	9·72	11·2	5·24	8·22	10·2	6·13
Nd	39·3	39·5	44·8	21·7	32·8	39·8	25·3
Sm	8·29	8·34	9·24	4·86	6·91	7·99	5·65
Eu	2·75	2·81	3·03	1·54	2·22	2·42	1·85
Gd	7·85	8·03	8·69	4·49	6·09	6·58	5·79
Tb	1·13	1·14	1·23	0·71	0·95	0·94	0·86
Dy	6·13	6·05	6·62	3·90	5·03	4·58	4·77
Ho	1·10	1·09	1·20	0·71	0·91	0·74	0·89
Er	2·66	2·62	2·88	1·80	2·28	1·70	2·23
Tm	0·35	0·35	0·39	0·24	0·30	0·20	0·30
Yb	2·14	2·07	2·35	1·46	1·80	1·15	1·88
Lu	0·30	0·29	0·33	0·20	0·25	0·15	0·26
Hf	5·50	5·07	6·49	2·79	4·50	4·24	3·66
Ta	3·48	3·29	3·85	1·63	2·87	3·36	2·00
W	0·41	0·69	0·67	n.a.	n.a.	n.a.	n.a
Tl	0·02	0·03	0·02	n.a.	n.a.	n.a.	0·01
Pb	2·37	2·10	2·71	3·26	2·24	2·45	3·52
Th	4·22	4·24	5·11	3·43	4·20	5·40	3·76
U	1·15	1·12	1·40	0·79	1·06	1·35	0·90

(continued)

Table 2: Continued

Sample:	MSI 17	MSI 20 B	MSI 20E	MSI 127A	MSI 128B	MSI 129A	NZS 8
Latitude (S):	43°38′04·7″	43°44′20·8″	43°44′20·8″	43°38′03·5″	43°37′35·3″	43°38′04·7″	43°41′33·9″
Longitude (E):	172°44′42·3″	173°04′14·1″	173°04′14·1″	172°43′22·3″	172°44′15·7″	172°44′42·3″	172°34′14·9″
Unit:	cd	sb; LBPI	sb; LBPI	sb	sb	cb	cd
Akaroa and Diamond Harbour Volcanic Groups							
Major elements (wt %; determined by XRF)							
SiO_2	47·56	49·44	42·29	48·73	48·77	46·06	42·27
TiO_2	2·91	2·34	2·85	1·92	1·98	2·89	2·99
Al_2O_3	17·68	17·94	12·26	14·10	14·08	17·01	14·33
FeO^t	11·92	12·07	13·17	11·25	11·21	12·00	12·55
MnO	0·18	0·18	0·18	0·16	0·16	0·18	0·17
MgO	4·23	2·02	11·51	9·54	8·91	4·40	7·58
CaO	7·97	5·64	10·74	9·35	9·51	7·88	10·76
Na_2O	4·67	4·30	3·77	3·02	3·29	4·75	2·69
K_2O	1·55	2·02	1·13	1·05	1·07	1·55	1·03
P_2O_5	0·74	1·20	0·71	0·37	0·39	0·71	0·49
CO_2	0·04	0·04	0·05	0·01	0·06	0·04	2·42
H_2O	0·62	3·04	0·78	0·50	0·64	0·77	0·86
Total	100·07	100·23	99·44	100·00	100·07	98·24	98·14
Trace elements (ppm; determined by ICP-MS)							
Li	6·46	8·17	6·23	8·60	7·48	7·36	14·1
Sc	9·56	7·67	24·1	22·2	24·1	9·79	21·1
V	131	51·8	284	205	223	136	286
Cr	7·74	0·52	517	310	352	9·35	203
Co	30·7	18·3	69·7	49·5	53·5	34·2	54·9
Ni	13·3	2·57	329	228	225	13·4	136
Cu	32·0	17·9	80·9	65·7	65·8	29·2	59·6
Zn	114	172	154	105	116	116	114
Ga	20·7	26·2	22·8	18·4	20·2	21·8	20·7
Rb	34·6	44·6	28·8	26·7	28·5	35·4	26·3
Sr	970	814	740	431	443	1091	672
Y	28·4	39·4	24·5	21·8	23·8	28·6	22·6
Zr	260	371	235	137	144	283	189
Nb	67·4	89·1	70·2	31·6	33·2	66·7	44·2
Mo	2·84	3·70	2·69	0·96	1·20	3·19	2·10
Cd	0·17	n.a.	n.a.	0·12	n.a.	n.a.	n.a.
Sn	1·98	2·63	1·88	1·38	1·54	1·96	1·61
Sb	0·07	0·06	0·07	0·06	0·06	0·08	0·06
Cs	0·49	0·32	0·64	0·57	0·40	0·45	3·36
Ba	439	619	438	270	268	349	542
La	43·9	62·3	48·4	22·2	23·0	42·8	30·4
Ce	89·6	112	95·3	45·3	46·1	83·2	61·9
Pr	10·6	15·6	12·0	5·79	6·01	10·5	7·62
Nd	42·0	60·4	47·3	24·1	24·5	40·8	31·0
Sm	8·54	11·9	9·50	5·36	5·49	8·26	6·68
Eu	2·82	3·90	2·99	1·76	1·79	2·74	2·22
Gd	8·07	10·8	8·52	5·43	5·46	7·66	6·43
Tb	1·14	1·52	1·15	0·81	0·81	1·08	0·93
Dy	5·99	8·08	5·67	4·43	4·51	5·74	4·96
Ho	1·07	1·47	0·93	0·81	0·84	1·03	0·89
Er	2·65	3·59	2·06	2·05	2·06	2·52	2·16
Tm	0·35	0·49	0·26	0·27	0·28	0·34	0·28
Yb	2·14	2·99	1·45	1·72	1·74	2·02	1·72
Lu	0·30	0·42	0·20	0·24	0·25	0·28	0·24
Hf	5·79	8·22	5·69	3·40	3·41	5·41	4·43
Ta	3·94	5·06	4·12	1·84	1·84	3·73	2·60
W	n.a.	0·61	0·89	n.a.	0·15	1·06	0·36
Tl	0·03	0·02	0·02	0·06	0·02	0·03	0·23
Pb	3·04	3·65	2·61	3·54	3·38	3·29	1·88
Th	5·40	7·12	5·67	3·46	3·50	5·73	3·35
U	1·40	1·90	1·46	0·80	0·78	1·51	0·92

Unit descriptions are after Sewell *et al.*, (1992). n.a., not analysed.

Table 3: Sr–Nd–Pb–Hf isotope ratios and $\delta^{18}O$ values

Sample	Group*	Unit**	$^{87}Sr/^{86}Sr$	2σ	$^{143}Nd/^{144}Nd$	2σ	$^{206}Pb/^{204}Pb$	2σ	$^{207}Pb/^{204}Pb$	2σ	$^{208}Pb/^{204}Pb$	2σ	$^{176}Hf/^{177}Hf$	2σ	‰ $\delta^{18}O$ (dupl)
Lyttelton volcano															
MSI 9A	HSG	lp	0·703067	3	0·512928	3	19.616	1	15.614	1	39.327	2	–	–	
MSI 10	HSG	l	0·703074	3	0·512912	3	19.536	3	15.601	2	39.241	5	–	–	4.76
MSI 107	HSG	l	0·703065	2	0·512924	2	19.406	1	15.594	1	39.162	2	0·283052	8	5.05
MSI 113	HSG	l	0·703220	4	0·512919	2	19.367	1	15.613	1	39.153	3	–	–	–
MSI 114	HSG	gd	0·704487	2	0·512780	2	19.107	1	15.642	1	38.793	2	–	–	–
MSI 125A	HSG	l	0·703663	3	0·512866	3	19.127	1	15.630	1	38.947	2	0·282972	9	5.19
MSI 130	HSG	l	0·705030	2	0·512745	3	19.065	1	15.635	1	38.905	2	–	–	–
MSI 131B	HSG	l	0·703359	3	0·512888	3	19.381	2	15.648	2	39.231	4	–	–	–
Mount Herbert Volcanic Group															
CD103	LSG	hh	0·703118	3	0·512959	3	19.633	1	15.606	1	39.336	2	–	–	4.81 (4.63)
M36B 2259	LSG	ho	0·703050	2	0·512956	2	19.444	2	15.596	2	39.171	4	–	–	4.76
MSI 117	LSG	hh	0·703025	3	0·512957	2	19.694	2	15.594	1	39.378	3	–	–	–
MSI 120	LSG	ho	0·703008	2	0·512967	2	19.563	1	15.579	1	39.239	3	–	–	4.73 (4.61)
MSI 134	LSG	hp	0·703086	3	0·512943	3	19.458	1	15.605	1	39.175	3	–	–	–
Akaroa Volcano															
N36C 3072	LSG	af	0·703025	3	0·512948	2	19.594	1	15.597	1	39.256	3	–	–	4.74
N36C 3602	LSG	af	0·703032	3	0·512957	2	19.502	1	15.602	1	39.207	2	–	–	–
UC 13809	LSG	af	0·702970	5	0·512965	3	19.622	2	15.587	2	39.279	4	–	–	–
MSI 18	LSG	af	0·703046	3	0·512956	3	19.619	2	15.590	2	39.281	5	–	–	4.86
MSI 144	LSG	ae	0·703124	3	0·512966	2	19.722	1	15.595	1	39.399	2	–	–	–
MSI 177	LSG	af	0·703031	3	0·512968	2	19.616	1	15.585	1	39.280	1	0·283048	6	4.65 (4.84)
Diamond Harbour Volcanic Group															
CD77	HSG	ds	0·703631	3	0·512863	2	19.141	2	15.636	1	38.992	3	–	–	–
CD112	LSG	ds	0·703056	3	0·512958	3	19.715	1	15.570	1	39.398	3	–	–	4.76
UC13790	LSG	LBPI (ds)	0·702993	2	0·512947	3	19.903	1	15.604	1	39.550	3	–	–	4.90
MSI 16	HSG	ds	0·703671	2	0·512853	3	19.101	1	15.630	1	38.943	2	–	–	–
MSI 17	LSG	cb	0·703062	3	0·512943	2	19.703	1	15.618	0	39.435	3	–	–	–
MSI 20E	LSG	LBPI (ds)	0·702998	3	0·512944	3	19.884	2	15.610	1	39.545	4	0·283036	5	4.80
MSI 127A	HSG	ds	0·703627	3	0·512866	3	19.118	4	15.625	3	38.958	8	0·282991	8	5.02
MSI 128B	HSG	ds	0·703592	3	0·512867	3	19.099	1	15.622	1	38.920	2	–	–	–
NZS8	LSG	cd	0·703027	6	0·512955	3	19.648	1	15.590	1	39.317	2	–	–	–

*HSG = high-silica group, LSG = low-silica group; **Unit descriptions are after Sewell *et al.* (1992).

related to the formation of the Akaroa volcano. Volcanic rocks from the youngest Diamond Harbour Volcanic Group show the widest range of compositions, varying from basanite through alkali basalt to tholeiite and mugearite (Fig. 2).

Based on the SiO_2 content, the moderately mafic (>4 wt % MgO) volcanic rocks can be grouped into a high-silica group (~>48 wt % SiO_2) and a low-silica group (~<48 wt % SiO_2; Figs 2 and 3a), although minor overlap between the two groups occurs. The more SiO_2-saturated volcanic rocks occur on the Lyttelton volcano, whereas the more SiO_2-undersaturated lavas occur on the Akaroa volcano. Exceptions include the Diamond Harbour volcanic rocks, which erupted on the Lyttelton shield, but have the geochemical characteristics of the low-silica Akaroa group volcanic rocks. In comparison with the high-silica Lyttelton volcanic rocks, the low-silica Akaroa volcanic rocks generally have higher contents of FeO^t, TiO_2, CaO, Sr and Nb but lower Pb for a given MgO content (Fig. 3b–g).

Incompatible element patterns for all mafic Banks Peninsula volcanic rocks on multi-element diagrams are strongly similar to those of ocean island basalts (Fig. 4), showing pronounced peaks at Nb–Ta and

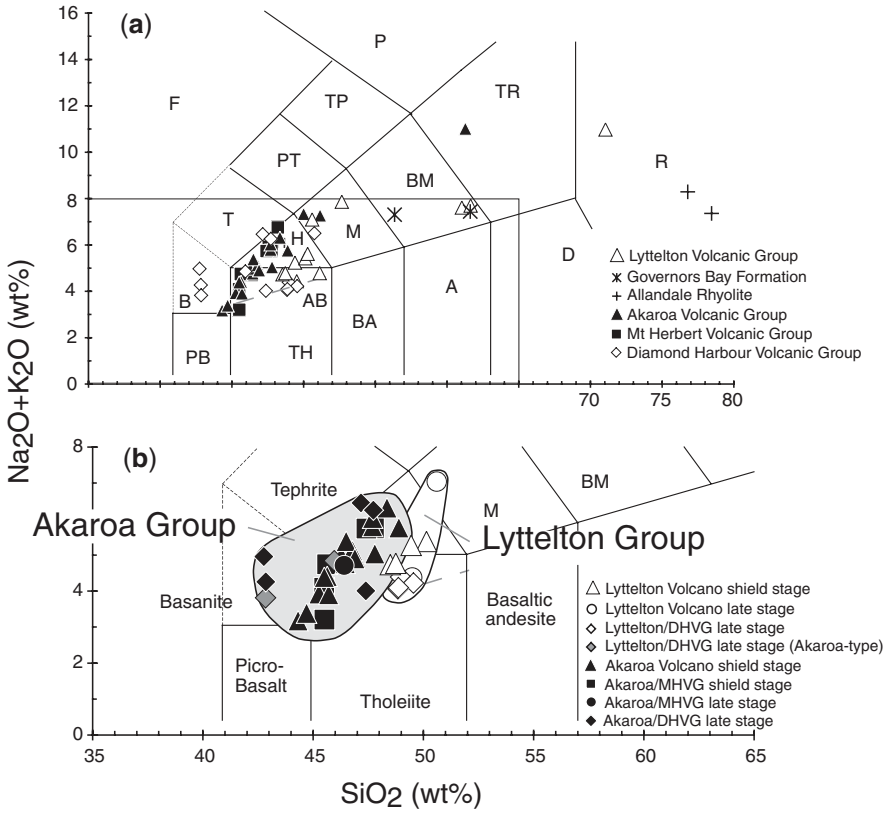

Fig. 2. (a) Total alkalis ($Na_2O + K_2O$) vs SiO_2 normalized to 100% on a volatile-free basis; boundaries according to Le Maitre (1989). Rock types range from basanite to transitional tholeiite through trachyte to rhyolite. Each symbol represents the assigned volcanic unit (Lyttelton, Mount Herbert, Akaroa and Diamond Harbour Volcanic Groups and the Governors Bay Formation and Allandale Rhyolite). Filled symbols represent units of the Akaroa Volcanic Group and open symbols units of the Lyttelton Group in all figures. The box in (a) shows the area enlarged in (b), which shows only mafic ($MgO > 4$ wt %) Banks Peninsula volcanic rocks. Based on the degree of SiO_2 saturation and on the spatial distribution, mafic Banks Peninsula lavas are grouped into a high-silica Lyttelton and a low-silica Akaroa Group. F, foidite; PB, picrobasalt; B, basanite; T, tephrite; PT, phono-tephrite; TP, tephri-phonolite; P, phonolite; TH, tholeiite; AB, alkali basalt; H, hawaiite; M, mugearite; BM, benmoreite; TR, trachyte; BA, basaltic andesite; A, andesite; D, dacite; R, rhyolite.

troughs for Pb and K. All samples are enriched in incompatible elements [large ion lithophile elements (LILE), light rare earth elements (LREE), high field strength elements (HFSE), Sr, U, Th, etc.] compared with mid-ocean ridge basalts (MORB) and have steep REE patterns [$(La/Yb)_N > 6{\cdot}5$, $(Sm/Yb)_N > 3{\cdot}5$ and $(Er/Yb)_N > 1$; N indicates normalized to primitive mantle after Hofmann (1988)] on multi-element diagrams. Akaroa lavas with low SiO_2 concentrations (basanites) have more pronounced peaks in Nb, Ta and Zr (higher Nb/La, Zr/Hf, Nb/Ta), and more prominent troughs for Pb and K. In the more silica-saturated Lyttelton volcanic rocks, ratios of fluid-mobile to less fluid-mobile incompatible elements [U/(Nb, La), (Rb, Ba)/Zr] are higher and ratios of more to less incompatible elements [such as Nb/Zr, (La, Sm)/Yb, Zr/Y, etc.] are lower. Exceptions are the late-stage high-silica lavas from Lyttelton volcano (Mount Pleasant Formation), which have more enriched incompatible element patterns (Fig. 4b).

Compared with normal Pacific MORB (P-MORB), the low-silica Akaroa group has more radiogenic Pb–Sr and less radiogenic Nd–Hf isotopic compositions with $^{206}Pb/^{204}Pb = 19{\cdot}44–19{\cdot}90$, $^{207}Pb/^{204}Pb = 15{\cdot}58–15{\cdot}62$, $^{208}Pb/^{204}Pb = 39{\cdot}17–39{\cdot}55$, $^{87}Sr/^{86}Sr = 0{\cdot}70297–0{\cdot}70312$, $^{143}Nd/^{144}Nd = 0{\cdot}51294–0{\cdot}51297$, $^{176}Hf/^{177}Hf = 0{\cdot}283036–0{\cdot}283048$ and $\delta^{18}O$ values of olivine of 4·65–4·90, below those common for mantle peridotite and MORB (Mattey *et al.*, 1994; Fig. 5). Their trace element and isotopic compositions suggest derivation from a source with a high time-integrated U/Pb ratio (i.e. a HIMU type mantle source). The high-silica Lyttelton group has generally higher $^{87}Sr/^{86}Sr = 0{\cdot}70307–0{\cdot}70367$, $^{207}Pb/^{204}Pb = 15{\cdot}59–15{\cdot}65$ and $\delta^{18}O$ values of 4·76–5·19, and generally lower $^{143}Nd/^{144}Nd = 0{\cdot}51285–0{\cdot}51293$, $^{206}Pb/^{204}Pb = 19{\cdot}10–19{\cdot}62$, $^{208}Pb/^{204}Pb = 38{\cdot}92–39{\cdot}33$ and $^{176}Hf/^{177}Hf = 0{\cdot}282972–0{\cdot}283052$ ratios (Fig. 5a–d) compared with the low-silica Akaroa volcanic rocks. Isotopic compositions extend from the Akaroa array towards an enriched (EMII-type) endmember.

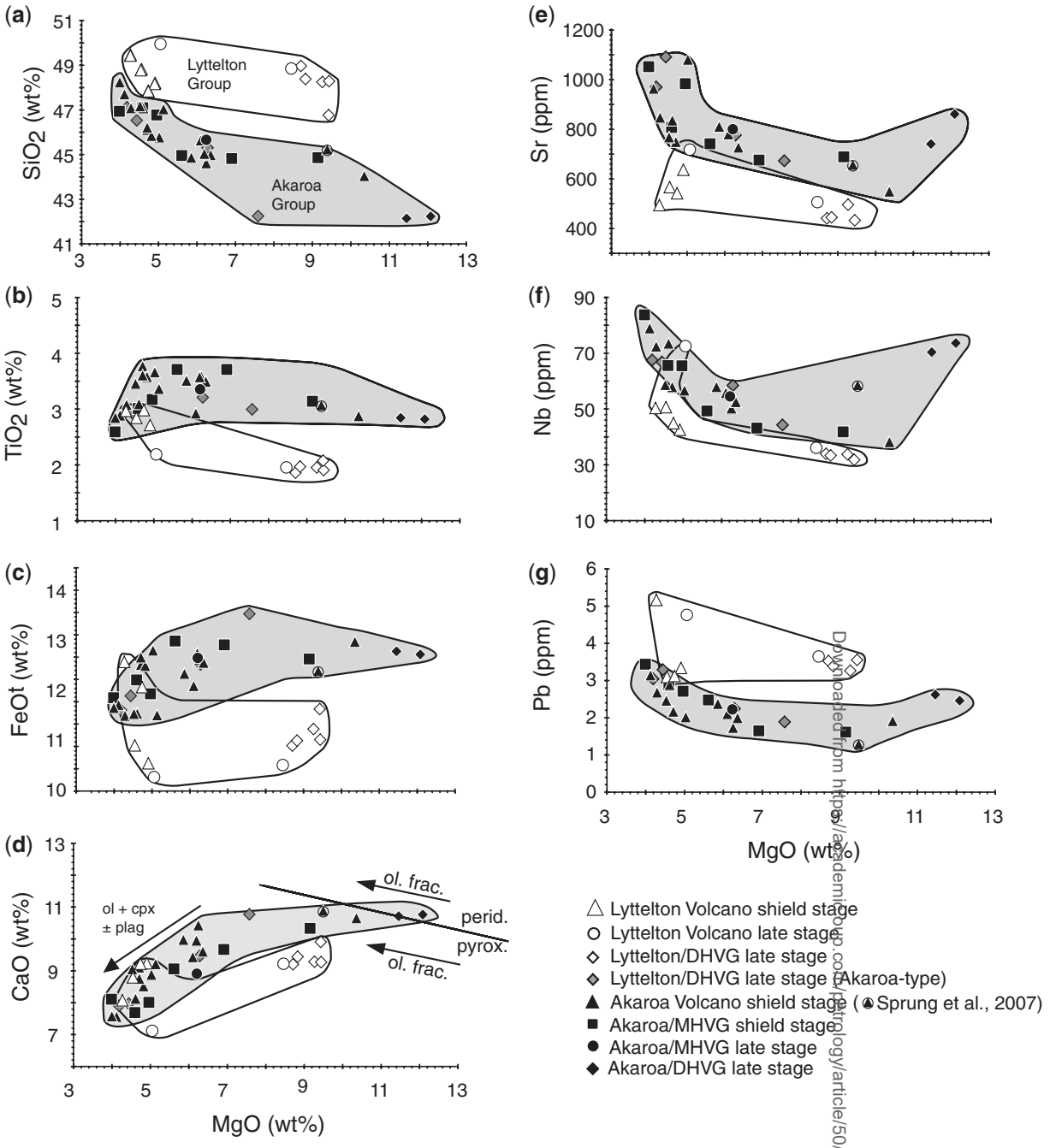

Fig. 3. (a–g) Diagrams showing selected major and trace elements vs MgO for mafic (MgO > 4 wt %) samples of the Banks Peninsula volcanic rocks. The two groups of samples from Lyttelton and Akaroa volcanoes define subparallel trends, with the Lyttelton group having higher SiO_2 and Pb, but lower TiO_2, FeO^t, CaO, Sr and Nb concentrations at a given MgO. The diagonal line in the MgO vs CaO diagram (d) represents the MgO/CaO (CaO = 13·81 − 0·274 MgO) division between peridotite and pyroxenite from Herzberg & Asimow (2008). The boundary divides the diagram into fields for melts derived from peridotitic (upper field) and pyroxenitic (lower field) sources. The black arrows represent crystal fractionation vectors, indicating fractionation of olivine (ol), clinopyroxene (cpx) ± plagioclase (plag). One additional data point from Sprung *et al.* (2007) was added (encircled triangle).

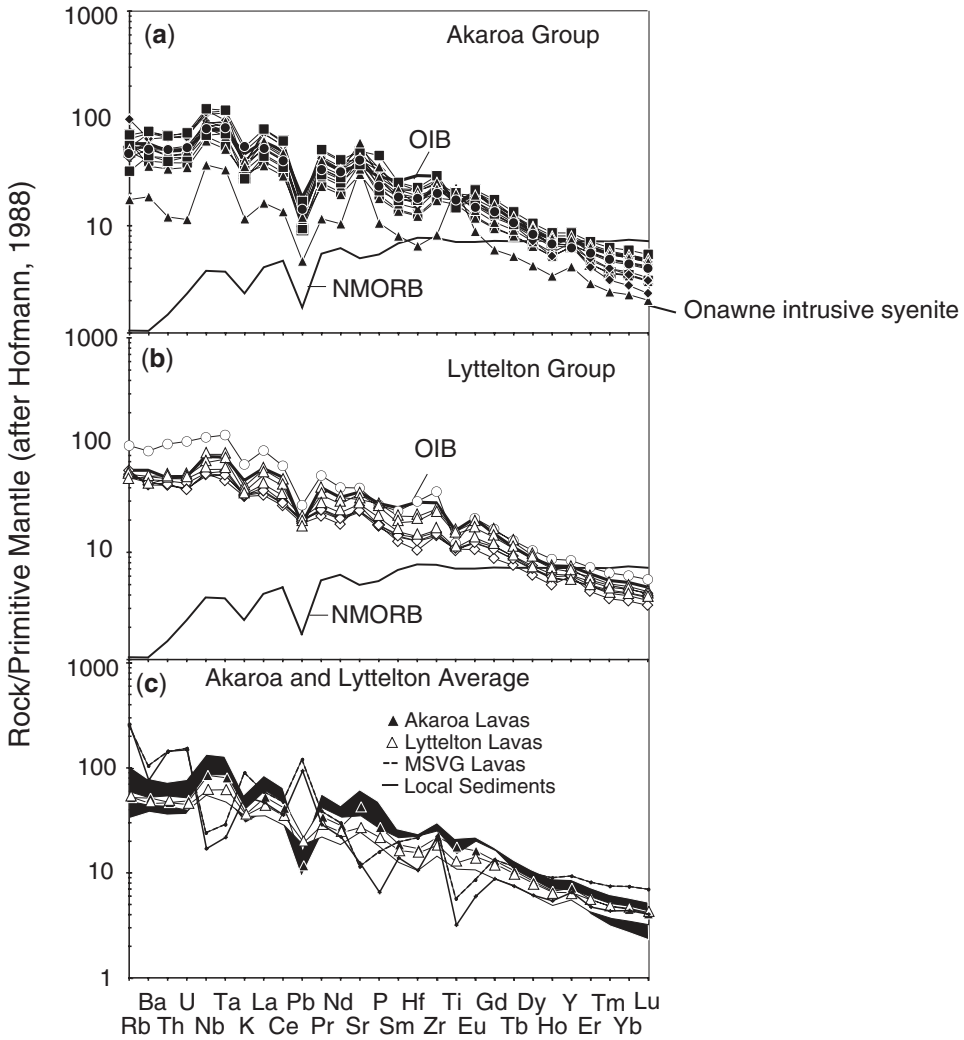

Fig. 4. Primitive mantle normalized (after Hofmann, 1988) incompatible element patterns of mafic lavas (MgO > 4 wt %) and the Onawne syenite on multi-element diagrams. All the volcanic rocks have incompatible element patterns similar to those of ocean island basalts and show enrichment in moderate and highly incompatible elements compared with MORB. Depletion in HREE, compared with MORB, indicates the presence of residual garnet in the source. Thick black lines represent typical OIB and N-MORB incompatible element patterns after Sun & McDonough (1989). Black and white shaded fields in (c) represent all mafic Akaroa and Lyttelton group lavas, respectively. The Akaroa group lavas have the most pronounced peaks for Nb and Ta, and troughs for K and Pb, which are less pronounced within the Lyttelton lavas. Although there is considerable overlap between Akaroa and Lyttelton group incompatible element patterns, the Akaroa Group samples trend towards slightly higher incompatible element contents compared with the Lyttelton rocks with similar MgO. The two fine dashed and solid lines in Fig. 4c represent incompatible element patterns of the average composition of the Mt. Somers Volcanic Group and the Torlesse sediments, outcropping on or near Banks Peninsula (data are taken from Tappenden, 2003).

DISCUSSION

Temporal and geochemical evolution of Banks Peninsula volcanoes

The temporal framework of volcanism on Banks Peninsula was previously based on K/Ar age determinations and stratigraphy (Sewell, 1988; Sewell *et al.*, 1993; Stipp & Mc Dougall, 1968; Weaver & Smith, 1989). The new $^{40}Ar/^{39}Ar$ ages presented here suggest that both volcanoes, Lyttelton and Akaroa, formed in two stages: (1) a voluminous shield stage; (2) a low-volume late stage (Fig. 6). Volcanic activity at Lyttelton presumably started with a fairly voluminous pulse of magmatism forming most of the Lyttelton volcano within ~1 Myr (12·5–11·5 Ma, including the Governors Bay Formation and the Allandale Rhyolite) by erupting a minimum of ~350 km^3 of shield lavas. After the shield stage, late-stage volcanic activity continued until ~10·5 Ma through the eruption of much lower volumes of mafic lava focused on the north flank of the Lyttelton volcano (the Mount Pleasant Formation), as well as dike intrusions varying from mafic to felsic in composition (Shelley, 1988).

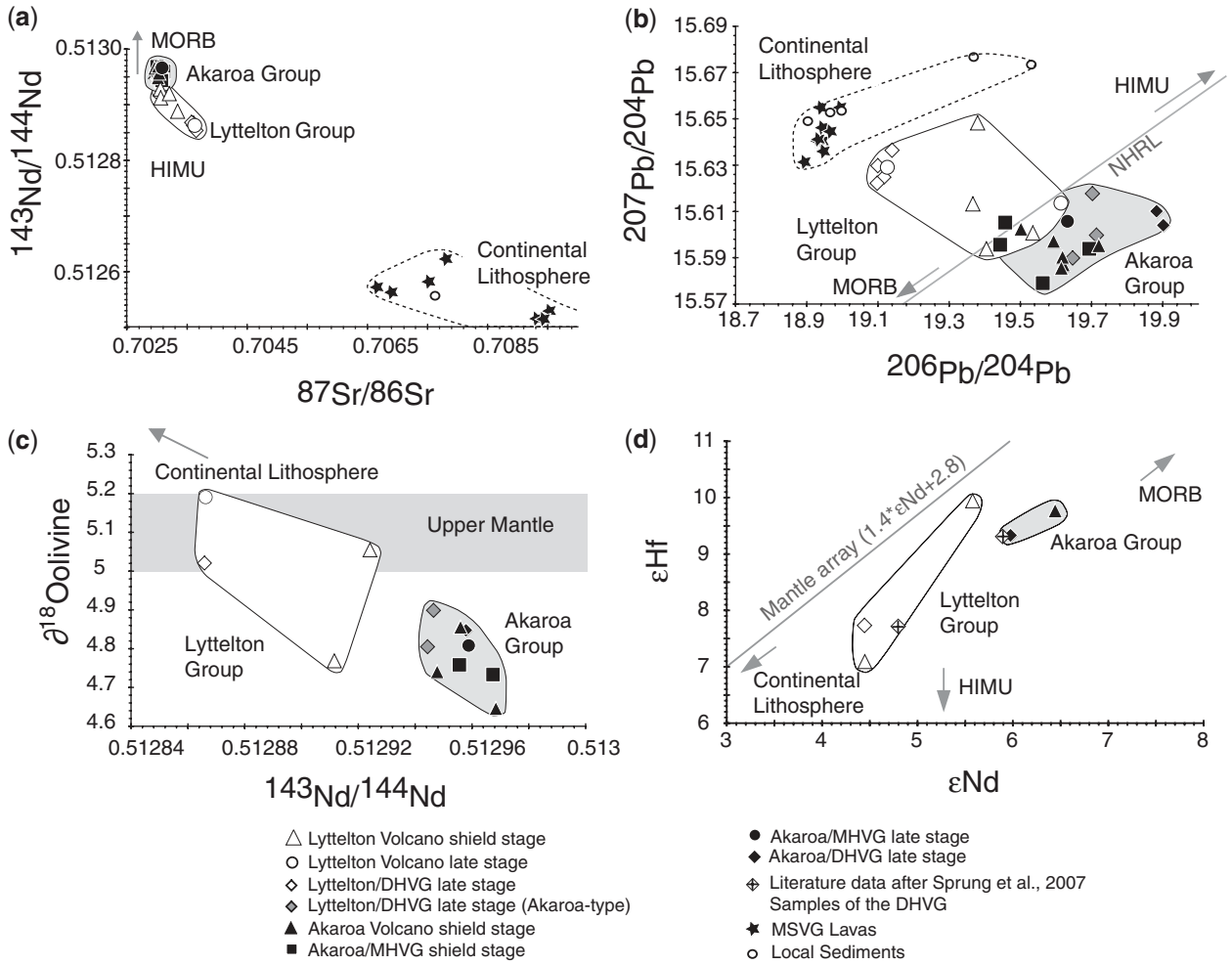

Fig. 5. (a–d) Sr, Nd, Pb, Hf and O isotopic compositions of mafic (MgO > 4 wt %) volcanic rocks from Banks Peninsula. Both Lyttelton and Akaroa volcanoes form isotopically distinct fields with minor overlap in Pb isotopic composition. The Akaroa group lavas have more radiogenic Pb–Sr and less radiogenic Nd–Hf isotopic compositions than MORB, trending towards the high time-integrated U/Pb (HIMU) component observed in OIB. The Lyttelton group lavas, compared with the Akaroa lavas, trend towards an enriched (EMII-type) endmember, which is represented by continental lithosphere [crust (white circles) and mantle (black stars); see text for details]. The grey rectangle in the Nd–O isotope diagram space represents the range in $\delta^{18}O$ for the common peridotitic upper mantle as defined by Mattey *et al.* (1994). The mantle array in the Nd–Hf diagram is based on data from Blichert-Toft & Albarede, 1997. Two additional data points (black crosses) in the Nd–Hf isotope diagram are taken from Sprung *et al.* (2007).

After a period of ~0·5 Myr of relative volcanic quiescence, volcanism shifted to the SE at ~9·6 Ma with the initiation of Akaroa volcano eruptions. The main volcanic edifice of the Akaroa volcano was formed within ~1 Myr (9·6–8·6 Ma) with more than three times the volume (~1200 km^3) of the Lyttelton volcano. The eruption products of the Akaroa shield-building stage were concentrated on the southeastern part of the peninsula; however, lower volumes of lava erupted from a centre situated on the deeply eroded SE flank of the Lyttelton volcano, forming the Mount Herbert Volcanic Group. After the shield stage of Akaroa volcano (including most of the Mount Herbert Group volcanic rocks), late-stage volcanism (Diamond Harbour Volcanic Group) continued for ~1·4 Myr (8·4–7 Ma) or 2·4 Myr [8·4–6 Ma, if the lower limit is based on the K/Ar ages of Sewell (1988)].

General geochemical characteristics of Banks Peninsula volcanic rocks

Broad correlations of MgO with other major and trace elements suggest that crystal fractionation played a role in the petrogenesis of each group (e.g. Fig. 3). Above MgO of ~8 wt %, Mg-rich olivine (forsterite) is the major fractionating phase, as indicated by its common presence as a phenocryst phase and the coupled decrease in MgO and Ni. Below 8 wt % MgO, the decrease in CaO and Cr, but increase in Al_2O_3 and Sr, with decreasing MgO is

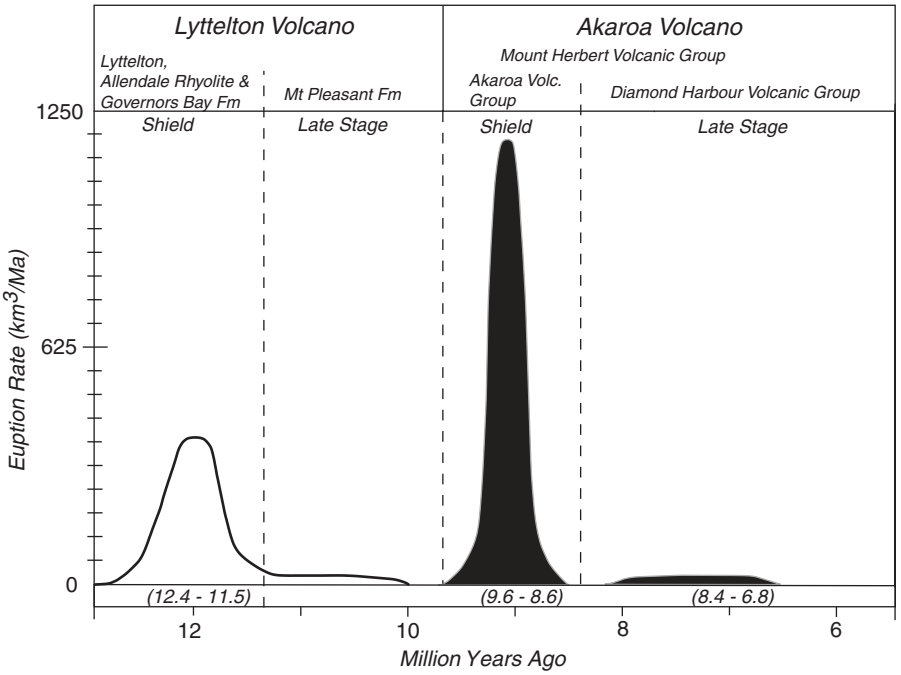

Fig. 6. Temporal evolution of the Banks Peninsula volcanism showing eruption rate vs $^{40}Ar/^{39}Ar$ age. Both volcanoes of Banks Peninsula, the older Lyttelton and the younger Akaroa volcano, formed rapidly (within ~1 Myr) during a voluminous shield-building stage (350 and 1200 km^3, respectively), followed by more protracted late-stage volcanism. Dashed lines divide the volcanic activity into shield and late stages. Peak volcanic activity occurred at ~12 Ma at Lyttelton and at ~9 Ma at Akaroa volcano.

consistent with the additional presence of clinopyroxene on the liquidus. A slight inflection in FeO^t and TiO_2 at MgO ~8 wt % in the Akaroa rocks argues for the onset of Fe–Ti oxide fractionation. Plagioclase phenocrysts are common in the hawaiites and mugearites of the Lyttelton Group (up to 30%), suggesting that plagioclase is also on the liquidus in these rocks.

A number of geochemical differences between the two groups at similar MgO contents, however, cannot be explained by fractional crystallization. Compared with the Lyttelton shield stage volcanic rocks, the Akaroa lavas have the following characteristics: (1) lower SiO_2, but higher FeO^t, CaO, TiO_2; (2) generally higher abundances of highly to moderately incompatible trace elements (e. g. Nb, Ta, Sr, etc.), but lower Pb (and Cs; not shown); (3) higher ratios of more to less incompatible elements [e.g. (La, Sm)/Yb, Sr/Y, Ta/Ce] and of Nb/Ta; (4) higher ratios of more to less fluid-mobile elements (e.g. Pb/Ce, U/Nb, Ba/La); (5) generally higher $^{206}Pb/^{204}Pb$, $^{143}Nd/^{144}Nd$ and $^{176}Hf/^{177}Hf$ but lower $^{87}Sr/^{86}Sr$ and $\delta^{18}O$. In general, the incompatible element compositions of the Banks Peninsula volcanic rocks are similar to those of ocean island basalts (OIB) (Fig. 4). The Akaroa Group volcanic rocks have HIMU-like isotopic compositions (although with more radiogenic Sr and less radiogenic Pb isotopic compositions than endmember HIMU from St. Helena or the Cook–Austral Islands), whereas the Lyttelton Group volcanic rocks tend towards a more enriched EMII-type isotopic composition.

Below we discuss the influence of crustal interaction, source composition and the origin of the low-silica (Akaroa) and high-silica (Lyttelton) groups.

Crustal interaction

The more enriched geochemical compositions of the Lyttelton volcanic rocks could in part reflect crustal interaction (Weaver & Sewell, 1986; Barley & Weaver, 1988); for example, assimilation of the Cretaceous Mount Somers Volcanic Group (McQueen's Andesites and Gebbies Pass Rhyolite; Tappenden, 2003) and/or Permian–Triassic Torlesse Group sedimentary rock, which crops out on the NW part of the Banks Peninsula.

Mixing of the most mafic low-silica Akaroa lavas with 7% Torlesse sediments or 20% Mt. Somers Volcanic Group lavas largely reproduces the major element contents of the most mafic, high-silica, Lyttelton lavas (<10% deviation). Such mixing (or assimilation), however, cannot explain many of the incompatible element characteristics of the Lyttelton basalts: specifically, the low TiO_2, U, Nb, Ta, LREE, Sr and Hf, and the high Na_2O and Pb (all >15% deviation), when mixing with Torlesse sediments, and the low TiO_2, K_2O, Pb, U, Th, Rb, Zr and Y, and high Na_2O, when mixing with Mt. Somers rocks (Table 4).

Quantitative calculation of the amount of fractional crystallization and assimilation of continental crust for Sr–Nd–Pb and O isotopes was conducted by using the energy constrained–assimilation fractional crystallization (EC-AFC) model of Bohrson & Spera (2001) and Spera & Bohrson (2001) (Figs 7a, b and 8a, b, and Table 5). Most of the Sr, Nd and Pb isotope compositions and $\delta^{18}O$ values of the enriched Lyttelton group lavas can be modeled by the addition of a crustal (EMII-type) endmember (Cretaceous Mount Somers Volcanic Group and/or Torlesse Group sediments) to the average isotope composition of the low-silica Akaroa volcanic rocks using the EC-AFC method. For the modeling, an initial temperature of ~1280°C was assumed for the most mafic high-silica Lyttelton lava (after Herzberg & Asimow, 2008); this represents the ascending magma, which then fuses surrounding 'continental-style' crust with a solidus temperature of ~900°C. If the temperature of the ascending (stagnating) low-silica magma drops below the solidus of the assimilant, no further interaction occurs. In the Sr–Nd, Nd–O and Pb–Pb isotope diagrams (Figs 7 and 8) allmost all of the high-silica Lyttelton samples can be generated by adding ≤10% local crustal material (Torlesse Group sediments) to a low-silica Akaroa-like magma. Mixtures of average Akaroa composition with Torlesse sediments to explain the lower trace element ratios (Ce/Pb, Nb/U, Nb/Th, Nb/La, Sr/Y and Sm/Yb) of the high-silica Lyttelton lavas (Fig. 9), however, require up to 35% assimilation of Torlesse sediments, inconsistent with the ≤10% assimilation required by the isotopic data. Most of the high-silica group volcanic rocks can also be explained through mixing of mafic low-silica Akaroa melts with *c.* 20–30% of the subduction-related Cretaceous EMII-type Mt. Somers volcanic rocks (Figs 7 and 8).

In conclusion, although mixing between crustal sediments and earlier subduction-related volcanic rocks with mafic, Akaroa low-silica melts can largely explain the major element compositions of the Lyttelton volcanic rocks, the fits for most incompatible elements are not very good (>15% deviation). In addition, it was not possible to derive the Lyttelton isotopic and trace element ratio compositions through mixing the same proportions of Akaroa melt and Torlesse sediments. Although crustal assimilation is likely to have influenced the composition of the Lyttelton magmas, especially the sample with the highest $^{207}Pb/^{204}Pb$, crustal assimilation alone (involving local crustal components) cannot explain the difference in composition between the low-silica Akaroa and the high-silica Lyttelton volcanic rocks. Therefore, we will now investigate potential differences in mantle source composition for the parental magmas of both of these volcanoes.

Source composition beneath Banks Peninsula

Arguments for the presence of recycled oceanic crust in the form of eclogite/pyroxenite in the source of mafic ocean island and other mafic intraplate basalts have largely been based on the trace element and isotopic composition of these rocks, in particular the presence of HIMU-type geochemical characteristics (e.g. Hofmann & White, 1982; Hofmann *et al.*, 1986; Zindler & Hart, 1986; Weaver, 1991). Recently. new techniques have been developed to assess the source lithology (peridotite vs pyroxenite/eclogite) of mafic volcanic rocks based on the chemistry of olivine phenocrysts and the major element composition of the volcanic rocks (e.g. Sobolev *et al.*, 2005, 2007; Gurenko *et al.*, 2008; Herzberg, 2006*a*, 2006*b*, Herzberg *et al.*, 2007, Herzberg & Asimow, 2008). Sobolev *et al.* (2005, 2007) proposed that high-silica melts derived from eclogite in a peridotitic matrix react with the surrounding peridotite to form pyroxenite and that olivines crystallizing from melts of the reaction pyroxenite will have high Ni but low MnO and CaO. Herzberg *et al.* (2006*a*) and Herzberg & Asimow (2008) pointed out that mafic rocks that have only fractionated olivine can be used to distinguish if the melts were derived from peridotite or pyroxenite sources on a MgO vs CaO diagram. On this diagram, peridotite-derived accumulated fractional melts plot above a line with the equation $CaO = 13{\cdot}81 - 0{\cdot}274\ MgO$, whereas many model pyroxenite-source melts plot below the line. Below we use the MgO and CaO contents of the most mafic Banks Peninsula lavas to assess whether they were derived from predominantly peridotitic or pyroxenitic sources.

The mafic (MgO > 8 wt %) low-silica Akaroa lavas with HIMU-type trace element and isotopic compositions have high CaO (plot above and slightly below the peridotite/pyroxenite dividing line of Herzberg & Asimow (2008) on the MgO vs CaO diagram; see Fig. 3d). Although some of the mafic Akaroa samples may have experienced some clinopyroxene in addition to olivine fractionation, this would have lowered the CaO content of the melts and may explain why the samples with lower MgO plot just beneath the boundary line. The major element composition of the most mafic samples (MgO > 11) is, however, consistent with partial melting of a primarily peridotitic source, rather than pyroxenite (or eclogite) as suggested by the HIMU-type trace element and isotopic compositions. On the other hand, the mafic high-silica Lyttelton lavas, which have no or minor clinopyroxene (≤1%), plot below the dividing line, implying derivation from a primarily pyroxenitic source; again, contrary to what was expected from the trace element and isotopic data. As has been demonstrated previously (e.g. Herzberg, 2006), it is not possible to derive the tholeiitic melts erupted from Lyttelton volcano through fractionation of the basanitic and alkali basaltic melts erupted from Akaroa volcano.

Table 4: Major and trace element mixing calculations

	Most mafic low-silica Akaroa lava N36C 3072	Assimilants		Av. high-silica Lyttleton Group; most mafic high-silica Lyttelton lavas	Modelled high-silica group composition by adding 7% sediment	Deviation (%)	Modelled high-silica group composition by adding 20% MSVG	Deviation (%)
		Av. Sediment composition*	Av. MSVG composition*					
Major elements in wt %								
SiO_2	44·0	70·0	59·3	48·5	45·9	5·52	47·1	2·96
TiO_2	2·87	0·578	1·41	1·93	2·71	−40·6	2·58	−33·7
Al_2O_3	13·1	15·1	16·2	14·1	13·3	6·09	13·7	2·65
FeO^t	13·4	4·26	7·25	11·0	12·7	−15·0	12·1	−9·71
MnO	0·181	0·049	0·111	0·155	0·170	−11·0	0·167	−7·90
MgO	10·4	1·34	3·52	8·95	9·73	−8·81	9·00	−0·567
CaO	10·6	1·68	5·62	9·28	10·0	−7·98	9·64	−3·91
Na_2O	2·37	4·02	3·44	3·11	2·49	20·2	2·58	17·0
K_2O	0·968	2·86	2·40	1·05	1·10	−4·78	1·26	−19·5
P_2O_5	0·393	0·142	0·344	0·398	0·376	5·56	0·383	3·65
Trace elements in wt %								
Rb	32·7	138	135	27·8	30·5	−9·79	53·2	−91·6
Ba	217	460	630	278	308	−10·7	299	−7·74
Th	2·74	11·7	11·5	3·62	3·94	−8·74	4·50	−24·2
U	0·707	3·01	3·10	0·848	1·02	−20·3	1·19	−39·8
Nb	38·0	10·5	14·8	33·7	49·6	−47·1	33·4	1·02
Ta	1·81	0·765	1·01	1·88	2·68	−42·6	1·65	12·0
La	22·2	28·7	36·2	23·4	31·3	−33·7	25·0	−6·78
Ce	46·6	56·9	75·9	47·3	63·9	−35·1	52·4	−10·9
Pb	1·91	16·4	20·9	3·48	2·42	30·3	5·72	−64·4
Nd	23·2	26·1	35·5	24·7	32·1	−30·1	25·7	−3·94
Sr	548	224	209	464	738	−59·1	480	−3·50
Sm	5·27	5·38	7·57	5·48	6·89	−25·9	5·73	−4·63
Hf	3·28	2·83	5·76	3·40	4·38	−28·6	3·77	−10·9
Zr	167	215	268	145	208	−43·3	187	−28·8
Eu	1·71	0·873	1·24	1·79	2·25	−25·9	1·62	9·30
Gd	4·83	4·51	6·84	5·41	6·43	−18·7	5·23	3·44
Tb	0·754	0·703	1·08	0·810	0·949	−17·3	0·820	−1·19
Dy	4·10	3·90	6·26	4·43	5·10	−15·1	4·53	−2·20
Y	25·0	25·8	36·7	23·0	27	−19·4	27·3	−18·9
Er	1·82	1·98	3·39	2·03	2·26	−11·2	2·13	−5·03
Tm	0·230	0·280	0·479	0·273	0·300	−9·73	0·280	−2·47
Yb	1·41	1·82	3·06	1·68	1·81	−7·76	1·74	−3·50
Lu	0·193	0·257	0·443	0·236	0·253	−7·20	0·243	−2·79

*Compositions of the assimilants are taken from Tappenden (2003). MSVG, Mt. Somers Volcanic Group.

To evaluate correlations between source composition, based on the major element data, and the trace element and isotopic data, we defined a peridotite/pyroxenite index $(= \mathrm{CaO} + (0.274 * \mathrm{MgO}) - 13.82)$ based on the deviation from the MgO/CaO division of Herzberg & Asimow (2008). Compositions plotting above the division in the peridotite source field have positive values and those below the line in the pyroxenite field have negative

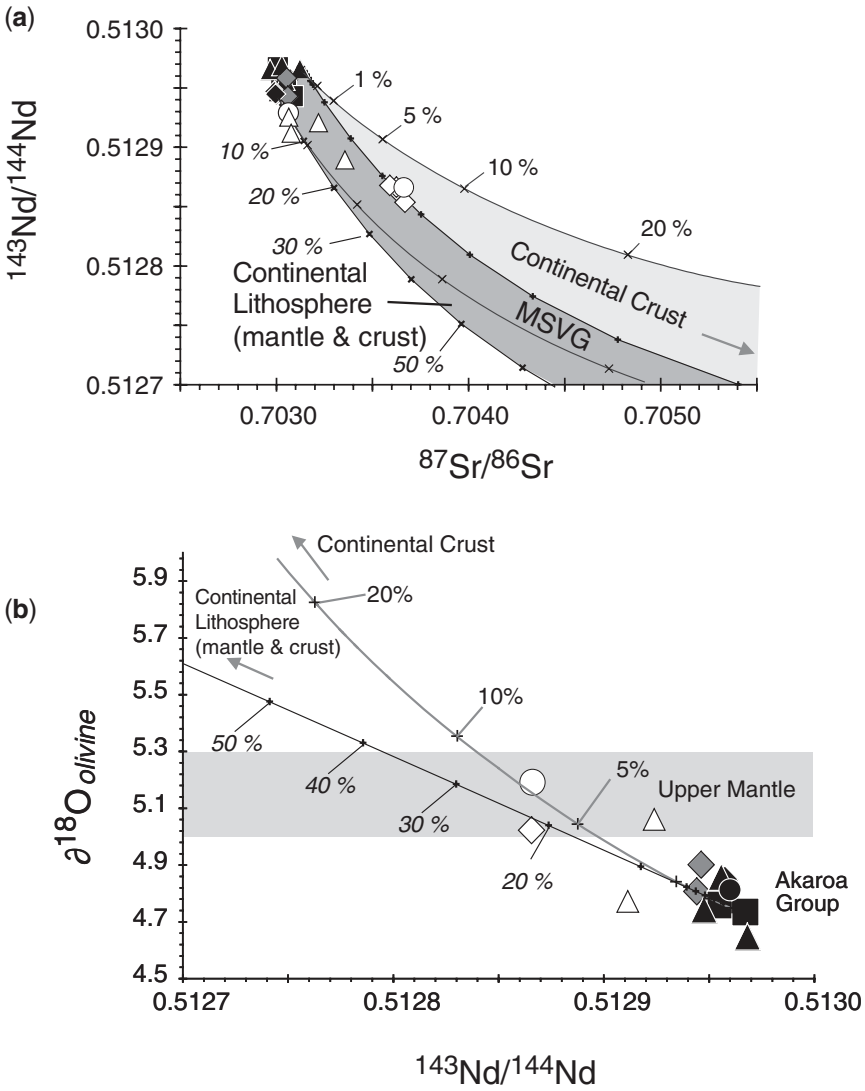

Fig. 7. (a, b) Sr, Nd and O isotope relationships of mafic (MgO > 4 wt %) Banks Peninsula volcanic rocks. The dark grey field represents mixing lines between the Akaroa group lavas and the Cretaceous, subduction-related volcanic rocks of the Mt. Somers Volcanic Group (MSVG) believed to be components in the lithosphere (mantle and crust) beneath Zealandia (this study). The light grey field represents an assimilation (mixing) trend [based on energy-constrained assimilation and fractionation modelling after Bohrson & Spera (2001) and Spera & Bohrson (2001)] between the Akaroa group lavas and the local continental crust on and around Banks Peninsula (see text for details). Tick marks on the edge of the light grey field represent percentage of local continental crust (Torlesse sediments) assimilated by Akaroa lavas, whereas the tick marks on the margin of the dark grey field represent the amount of the Mt. Somers volcanic rocks mixed into the Akaroa lavas. For the Mt. Somers arc endmember, a $^{143}Nd/^{144}Nd$ value of 0·51257 (Tappenden, 2003) and a $\delta^{18}O = 6{\cdot}2$ [average for continental arc basalts after Harmon & Hoefs (1995)] were chosen. Endmember compositions of the local continental crust are taken from Tappenden (2003).

values. Interestingly, there are good to excellent correlations ($r^2 \geq 0{\cdot}7$, except for $\delta^{18}O$ with $r^2 = 0{\cdot}6$; Fig. 10a–l) of the peridotite/pyroxenite index with major and trace elements and with trace element and isotope ratios for the mafic volcanic rocks from Banks Peninsula. The peridotite/pyroxenite index exhibits positive correlations with FeO^t, TiO_2, MnO, Cr, Zr, Sr, $(Sm, Gd/Yb)_N$, (Ce, Nd)/Pb, Nb/(U, Th, La) $^{206}Pb/^{204}Pb$, $^{208}Pb/^{204}Pb$, εNd and εHf, and negative correlations with SiO_2, Al_2O_3, $^{87}Sr^{86}Sr$, $^{207}Pb/^{204}Pb$ and $\delta^{18}O$. The good to excellent correlations suggest that the major element, trace element and isotopic composition of the Banks Peninsula melts are controlled by mixing of melts from two distinct sources, possibly reflecting differences in source lithology (peridotite vs pyroxenite).

Together with the low CaO contents of the mafic high-silica Lyttelton lavas, the low MnO and Cr are also consistent with derivation from a pyroxenitic rather than a peridotitic source, because these oxides or elements are more compatible in orthopyroxene than in olivine and

Table 5: Modelling parameters for energy-constrained assimilation–fractional crystallization (EC-AFC) calculations after Bohrson & Spera (2001) and Spera & Bohrson (2001)

EC-AFC Parameters			
	Thermal Parameters		
Magma liquidus temperature	1280°C	Crystallization enthalpy (J/kg)	396000
Magma initial temperature	1280°C	Isobaric specific heat of magma (J/kg per K)	1484
Assimilant liquidus temperature	1000°C	Fusion enthalpy (J/kg)	270000
Assimilant initial temperature	650°C	Isobaric specific heat of assimilant (J/kg per K)	1370
Solidus Temperature	900°C		
Equilibration Temperature	980°C		

		Compositional Parameters				
Element		Sr	Nd	Pb	Pb	O
Magma initial concentration (ppm)	Magma 1 (MSI 144)	1080	38·5	2·01	2·01	0·47
	Magma 2 (MSI 20E)	740	47·3	2·61	2·61	
Bulk D0 in magma		1·0	0·25	0·1	0·1	
Enthalpy of trace element distr. Magma		0	0	0	0	
Assimilant initial concentration	Assimilant 1*	391	21·0	7·67	7·67	0·5
	Assimilant 2*	126	22·8	17·3	17·3	
Bulk D0 in assimilant		0·5	0·25	0·1	0·1	
Enthalpy of trace element distr. Assim.		0	0	0	0	
Isotope ratio/∂^{18}O value in magma	Magma 1 (MSI 144)	0·702998	0·512944	19·88	15·61	4·8
	Magma 2 (MSI 20E)	0·703124	0·512966	19·56	15·58	
Isotope ratio/∂^{18}O value in assimilant	Assimilant 1*	0·707680	0·512558	19·53	15·67	8·8
	Assimilant 2*	0·716264	0·512381	18·90	15·65	

Results are displayed in Fig. 7a–b and 9a. *Data for the crustal assimilants are taken from Tappenden (2003). The ∂^{18}O value of 4.8 of the magma represents the average ∂^{18}O value of the low-silica group lavas

thus are retained in the source if orthopyroxene remains in the residuum (Sobolev *et al.*, 2007, and references therein). The higher CaO, MnO, Cr contents in the low-silica Akaroa lavas are consistent with derivation from a peridotitic source. We note, however, that slightly greater amounts of fractionation of the high-silica Lyttelton lavas could have reduced the Cr and Ni contents of these lavas, making interpretations based on these elements tenuous.

Low Al_2O_3 and high $(Sm/Yb)_N$ ratios in the low-silica group volcanic rocks suggest greater amounts of residual garnet in the source, which could reflect more garnet originally in the low-silica source, lower degrees of melting of the low-silica source or greater pressures (depths) of melting (within the garnet stability field versus the spinel stability field or at the border of the two stability fields) to generate the low-silica rocks. Pressure has a significant effect on the SiO_2 and FeO^t content of partial melts of volatile-free peridotite at pressures less than 30 kbar (e.g. Hirose & Kushiro, 1993) and therefore the lower SiO_2 and higher FeO^t of the Akaroa rocks could possibly also reflect greater melting pressures (depths) if the high-silica Lyttelton melts were formed at pressures less than 30 kbar (<100 km depth). Experiments on natural carbonated peridotite, however, have shown that melts from carbonated peridotite have low SiO_2 and high CaO and can have high MgO and FeO^t contents (Hirose, 1997; Dasgupta *et al.*, 2007*a*), indicating that derivation from carbonated peridotite may also have influenced the major element composition of the Akaroa melts. The compositions of the most mafic Lyttelton lavas, however, plot to the right of the boundary proposed by Herzberg & Asimov (2008) to distinguish melts formed from carbonated peridotite (left of the boundary) and those that are not (right of the boundary) on a SiO_2 vs CaO diagram (the boundary being given by $CaO = 2{\cdot}318\ SiO_2 - 93{\cdot}626$), consistent with the Lyttelton melts being derived from pyroxenite.

Finally, we note that lower (Ce, Nd)/Pb, Nb/(U, Th), and (Nb, Ta)/(La, Sm) in the Lyttelton lavas reflect a higher influence of a subduction-related component [higher quantities of fluid-mobile elements (U, Pb), more sediment contribution (Th, Pb) and relative depletion in Nb and Ta] in the pyroxenitic souce component, compared

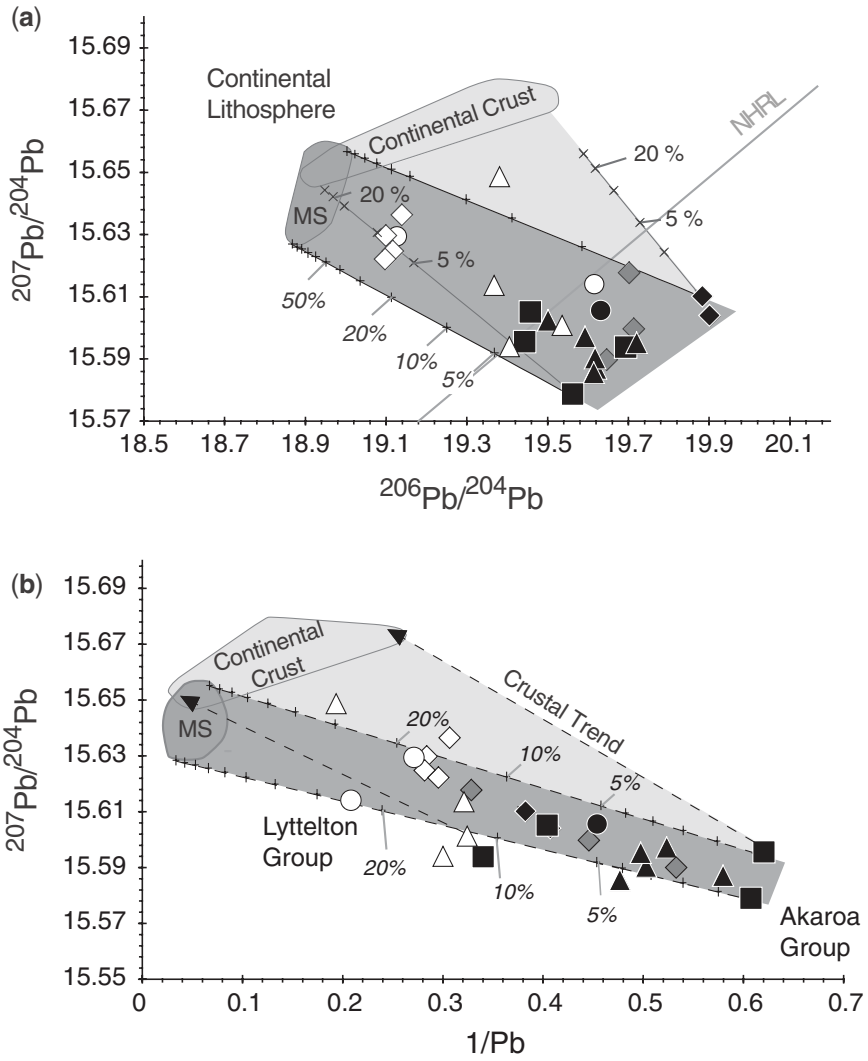

Fig. 8. (a–b) $^{206}Pb/^{204}Pb$ vs $^{207}Pb/^{204}Pb$ and 1/Pb vs $^{207}Pb/^{204}Pb$. Light grey field represents mixtures that can be produced through mixing of Akaroa parental basalt and Torlesse crustal rocks, whereas the dark grey field represents mixtures with Mt. Somers volcanic rocks (see Fig. 11a and b). Tick marks represent the amount of these lithospheric components assimilated (mixed) with the Akaroa group lava. NHRL, northern hemisphere reference line.

with the peridotitic component. In summary, the correlations between the peridotite/pyroxenite index and the major and trace element and isotopic composition suggest that the low-silica HIMU-type Akaroa lavas were derived primarily from a peridotitic source and the high-silica, EMII-type Lyttelton lavas from a pyroxenitic source. Considering that HIMU-type trace element and isotopic signatures are generally intepreted to reflect the presence of recycled oceanic crust in the form of eclogite or pyroxenite in the source of these magmas, it is rather surprising that their major element compositions suggests derivation from carbonated peridotite instead. Similar evidence for the HIMU-type signature in melts derived from peridotite was found in lavas from the Cook–Austral Islands (Herzberg, 2006*b*) and the Canary Islands (Gurenko *et al.*, 2008). Gurenko *et al.* (2008) proposed that the HIMU-type signature was derived from old (>1 Ga) recycled oceanic crust stirred (by mantle convection) into and/or reacted with the depleted upper mantle. We, however, propose an alternative explanation below.

Low-silica group: HIMU-type carbonated peridotite melting in upwelling asthenosphere

Although some major and trace element data point to a carbonated peridotitic source for the low-silica Akaroa volcanic rocks, the incompatible element concentration patterns and isotopic data point to an input from recycled oceanic crust in the form of carbonated eclogite or

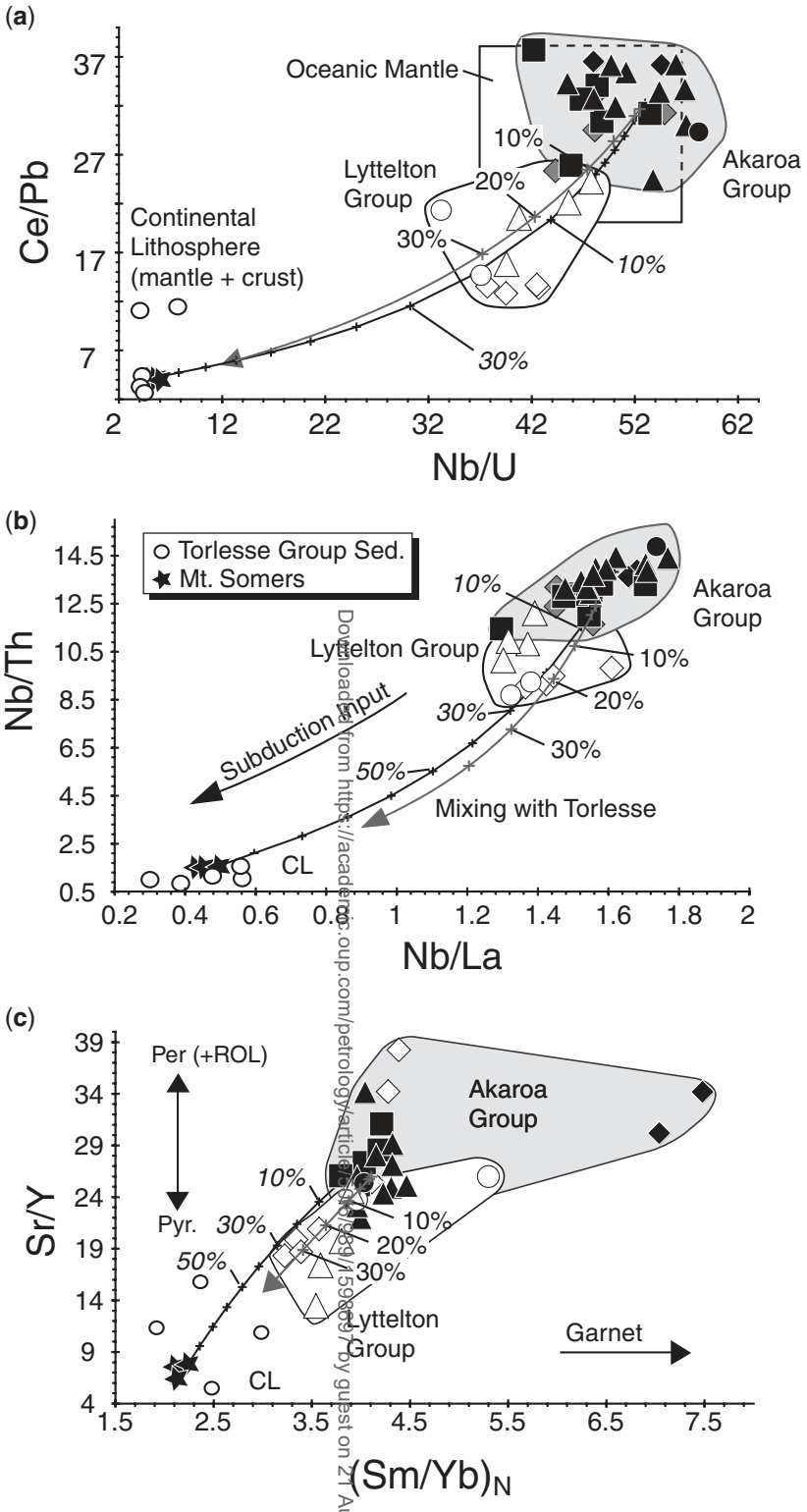

Fig. 9. (a–c) Selected trace element ratios of the moderately mafic (MgO > 4 wt %) volcanic rocks from Banks Peninsula. (a) Ce/Pb vs Nb/U indicates the involvement of at least two different mantle sources for the low and high silica groups. The white rectangle of the 'oceanic mantle' represents the Ce/Pb and Nb/U values taken from Hofmann (2006) and Hofmann *et al.* (1986). The white circles represent Torlesse Group sediments and the black stars represent mafic (MgO > 5 wt %) subduction-related Mt. Somers volcanic rocks (this study; Tappenden, 2003). (a–c) Low Ce/Pb, Nb/(U, Th, La) and Sr/Y are commonly found in crustal and arc-related rocks, suggesting mixing between either of these compositions and low-silica Akaroa volcanic rocks to derive the high-silica Lyttelton volcanic rocks. (c) $(Sm/Yb)_N$ displays an increasing garnet signature with decreasing SiO_2 (wt %). Black curved lines with tick marks represent binary mixing between average low-silica Akaroa volcanic rocks and the Mt. Somers Volcanic Group. The curved gray line with arrowhead represents mixing between low-silica Akaroa rocks and Torlesse Group sediments. To generate the trace element ratios (shown in a–c) of the Lyttelton high-silica volcanic rocks *c.* 20–30% of the Mt. Somers and *c.* 5–35% Torlesse sediments need to be mixed with an average low-silica Akaroa group lava. CL, continental lithosphere; ROL, recycled oceanic lithosphere.

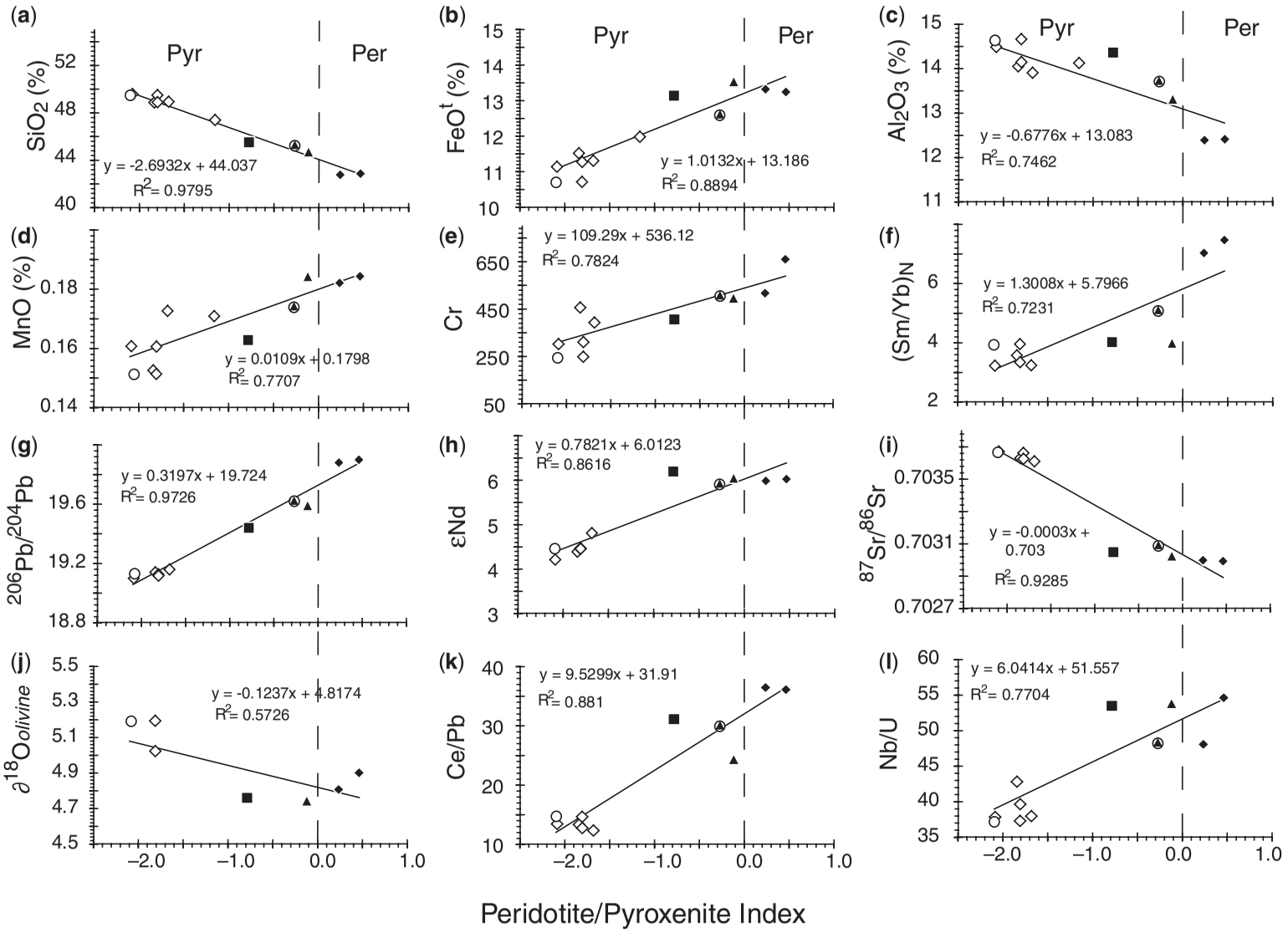

Fig. 10. (a–l) Peridotite/pyroxenite index [= CaO + (0·274 MgO) − 13·81, reflecting deviation from the dividing line between peridotite and pyroxenite fields on the MgO vs CaO diagram of Herzberg & Asimow (2008)] versus selected major and trace element and isotope data for mafic volcanic rocks (MgO > 8 wt %) from Banks Peninsula. The systematic correlations of major and trace elements and Sr–Nd–Pb–O with peridotite/pyroxenite index (essentially an index of whether the melts are derived predominantly from peridotite or pyroxenite sources) are consistent with the derivation of the low-silica volcanic rocks through partial melting of peridotite and the high-silica volcanic rocks through melting of a primarily pyroxenitic component.

pyroxenite. Over the last few years, high-pressure melting experiments have demonstrated that silica-poor mafic melts, common in intraplate volcanic settings, can be produced by partial melting of either carbonated peridotite (Hirose, 1997; Dasgupta *et al.*, 2007*a*, 2007*b*) or pyroxenite and/or carbonated eclogite (e.g. Hirschmann *et al.*, 2003; Dasgupta *et al.*, 2006; Kogiso & Hirschmann, 2006). High $(Sm/Yb)_N$ (3·5–7·6; Fig. 9c) and Nb/Ta (16·7–21·5) in the mafic Akaroa lavas are consistent with residual Ca-rich garnet in the source. Ca-rich (eclogitic) garnet incorporates Yb and Ta preferentially to Sm and Nb, resulting in increased Sm/Yb and Nb/Ta in the melts derived from such a source (Pfänder *et al.*, 2007). High Sr/Y (>21, Fig. 9c), which is also high in adakitic magmas derived from eclogite melting (Bindeman *et al.*, 2005), is also consistent with a contribution from an eclogitic component. Furthermore, the high FeO^t, TiO_2, Nb/La and Nb/Ta can also reflect the presence of rutile and/or titanite, which are common phases in eclogite (Yaxley & Green, 1994; Rudnick *et al.*, 2000; John *et al.*, 2004; Schmidt *et al.*, 2004). The incompatible trace element (Fig. 4) and long-lived radiogenic isotope ratios of Sr, Nd, Hf and Pb (Fig. 5) have HIMU-type signatures. Such compositions are not consistent with derivation of the low-silica Akaroa rocks from depleted upper mantle peridotite, but instead display a signature characteristic of hydrothermally altered recycled oceanic crust (e.g. Hofmann & White, 1982; Hoernle *et al.*, 1991, 2006). The low $\delta^{18}O$ of 4·6–4·9 measured in olivine from the Akaroa lavas is below the average mantle value of $5·2 \pm 0·2$ ‰ (Mattey *et al.*, 1994), altered upper basaltic oceanic crust ($\delta^{18}O = 5–9$) and pelagic sediments ($\delta^{18}O = 15–25$; Eiler, 2001), but characteristic of hydrothermally altered lower gabbroic crust and altered peridotite ($\delta^{18}O = 3–5$). Therefore the incompatible element concentrations and isotopic data point to the involvement of metamorphosed, hydrothermally altered, lower oceanic crust in the form of eclogite in the formation of the Akaroa lavas, as has also been proposed for ocean island volcanic rocks; for example, from the Canaries, Madeira and Azores (Hoernle *et al.*, 1998; Geldmacher & Hoernle, 2000; Turner *et al.*, 2007).

The Pb isotopic compositions of the Akaroa volcanic rocks fall between endmember HIMU (from St. Helena and the Cook–Austral Islands) and N-MORB, which could reflect relatively young HIMU recycling ages for the oceanic lithosphere (e.g. Hoernle *et al.*, 2006) or mixing between HIMU and DMM sources. Assuming a slightly depleted DMM composition [$^{206}Pb/^{204}Pb \sim 18$ (Workman & Hart, 2005); Pb ~ 0·5 ppm and $\delta^{18}O \sim 5$‰ (lower value after Mattey *et al.*, 1994)], then the addition of ~8–20% of a ~0·7–1·3 Ga lower recycled oceanic crust (assuming $\mu = 15$, Pb = 20 ppm and $\delta^{18}O = 3·3$‰, after Hansteen & Troll, 2003) could explain the Pb and O isotope compositions of the mafic low-silica, volcanic rocks from the Banks Peninsula (Fig. 11). Therefore the source of the Akaroa mafic lavas could be primarily peridotitic containing ~8–20% eclogite, with the eclogitic component dominating the incompatible element contents and thus significantly affecting the Sr–Nd–Pb–Hf isotopic compositions.

As noted above, Gurenko *et al.* (2008) explained derivation of Canary Island volcanic rocks from a HIMU-type of peridotitic mantle source through complete stirring of the eclogite into the peridotitic matrix. The recent melting models of Dasgupta *et al.* (2006, 2007*a*) provide an alternative scenario for explaining a HIMU-type of peridotitic source. If the upwelling asthenospheric mantle beneath Banks Peninsula contains carbonated eclogite (*c.* 0·7–1·3 Ga recycled ocean crust/lithosphere) in a peridotitic matrix, then the eclogite will cross its solidus at the greatest depth, melting to form carbonatitic or carbonate-rich low-silica partial melts (Fig. 12). These melts, rich in incompatible trace elements and possibly also in FeO^t and TiO_2 (Dasgupta *et al.*, 2006) could metasomatize the surrounding depleted upper mantle peridotite, imparting the geochemical characteristics (incompatible trace element and isotopic composition) of the eclogite on the depleted peridotite. When the carbonated peridotite crosses the solidus at shallower depths, it could produce melts with compositions similar to the mafic Akaroa volcanic rocks (Fig. 12).

High-silica group: lithospheric melting

As summarized above, the Lyttelton group volcanic rocks have higher SiO_2, Pb and Cs but lower Nb, Ta, (Ce, Nd)/Pb, (Nb, Ta)/(U, Th, Ba, Rb, La) (Fig. 10a–c) compared with Akaroa group volcanic rocks with similar MgO contents. In addition, the Lyttelton volcanic rocks generally have higher $^{207}Pb/^{204}Pb$, $^{87}Sr/^{86}Sr$ and $\delta^{18}O_{olivine}$ (although they do not exceed the common mantle values) and lower $^{206}Pb/^{204}Pb$, $^{143}Nd/^{144}Nd$ and $^{176}Hf/^{177}Hf$, or an EMII-type isotopic signature. As discussed above, the derivation of the high-silica Lyttelton magmas from subduction-related pyroxenitic cumulates and/or veins in the lithosphere, which have similar isotopic but different major and trace element compositions to the Mt. Somers Volcanic Group lavas, could, at least in part, explain the variations in major and trace element composition. Partial melts of pyroxenites can be low in TiO_2, K_2O, Pb, U, Th, Rb, Zr, Y (and REE) (e.g. Herzberg, 2006*a*; Downes, 2007). The higher Na_2O in the high-silica Lyttelton lavas could reflect derivation from an Na-enriched pyroxenitic source with $D_{Na}^{cpx/melt}$ of ~1 (Pertermann & Hirschmann, 2002; Elkins *et al.*, 2008).

It has been shown that historical tholeiitic basalts erupted on the Canary Islands can be formed by mixing of an asthenospheric low-silica melt with a high-silica lithospheric melt in proportions of 40–60%. The high-silica lithospheric melt can be formed by

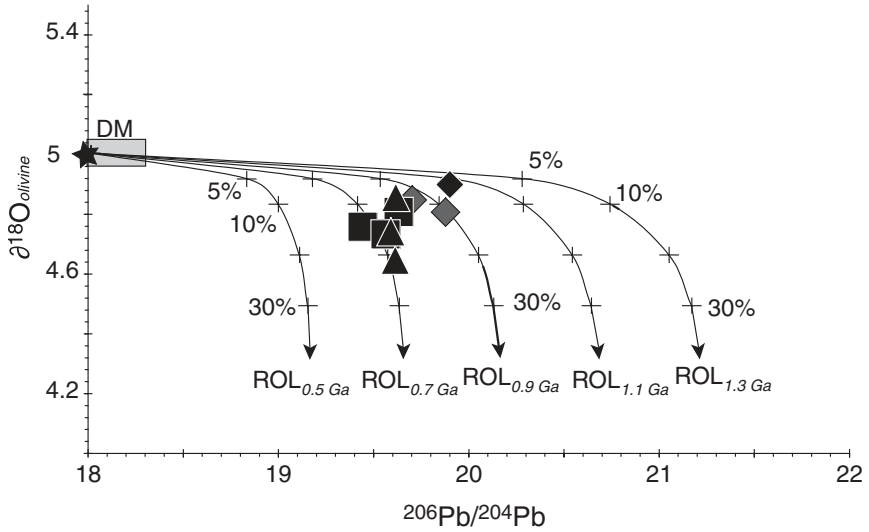

Fig. 11. $^{206}Pb/^{204}Pb$ vs $\delta^{18}O_{olivine}$ for the moderately mafic (MgO > 4 wt %), low-silica volcanic rocks from the Banks Peninsula. The grey rectangle indicates the Pb isotopic composition of depleted (MORB-source) mantle (DM). Mixing curves depict mixing of depleted mantle (black star) with 0·5, 0·7, 0·9, 1·1 and 1·3 Ga recycled oceanic lithosphere (ROL). The compositions of the mixing endmembers are as follows. DM: $^{206}Pb/^{204}Pb = 18$ (Workman *et al.*, 2005), $\delta^{18}O_{olivine} = 5$ (lower value of Mattey *et al.*, 1994), Pb = 0·5 ppm. ROL: $\mu = 15$; Pb = 20 ppm, $\delta^{18}O_{olivine} = 3{\cdot}3$ (Hansteen & Troll, 2003). To explain the Pb and O isotopic composition of the low-silica volcanic rocks from Banks Peninsula, a mixture of *c.* 8–20% of *c.* 0·7–1·3 Ga ROL with 80–92% DM is required.

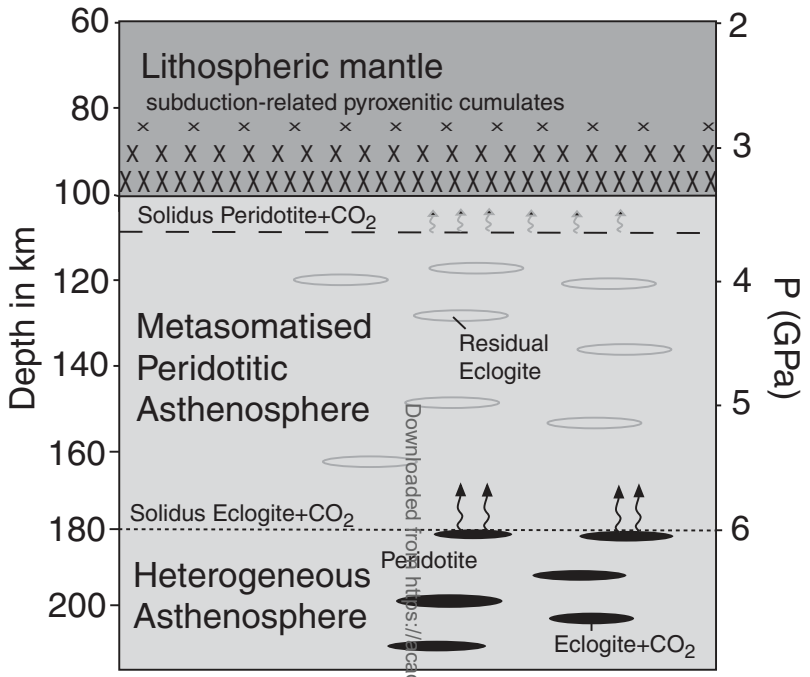

Fig. 12. Schematic illustration showing the depth of partial melting of carbonated eclogite and carbonated peridotite in the upper asthenosphere beneath Banks Peninsula. The depth estimate of ≤180 km for incipient partial melting of eclogite + CO_2 (recycled oceanic lithosphere) is derived from the FeO^t content of the most mafic volcanic rocks of the low-silica Akaroa group from Banks Peninsula, following Herzberg *et al.* (2007). The depth estimate of ≤110 km for partial melting of carbonated peridotite is from Dasgupta *et al.* (2007*a*). The carbonated eclogite (recycled lower oceanic crust) partially melts by decompression at ≤180 km and metasomatizes the surrounding depleted (MORB source) upper asthenosphere, which then melts at ≤110 km.

diffusive infiltration of alkalis from ascending low-silica basanitic melts into the lithospheric mantle, causing incongruent melting of orthopyroxene (Lundstrom *et al.*, 2003). Assuming a strongly metasomatized lower lithosphere (e.g. as a result of subduction along the Gondwana margin), similar processes could account for the formation of the high-silica Lyttelton lavas. The EMII-type lavas of the Mt. Somers Volcanic Group are also likely to reflect the composition of at least parts of the lithospheric mantle. Because the high-silica melts appear to be derived from a pyroxenitic source component (as discussed above), subduction-related Mt. Somers volcanic rocks may have crystallized as pyroxenitic cumulates within the lithosphere (both crust and mantle) beneath Lyttelton volcano (Fig. 10a–l). Melting of these cumulates during the late Miocene could have contributed to the compositional differences between the Akaroa (largely asthenospheric melts) and the Lyttelton (largely lithospheric) melts.

The late-stage volcanic rock MSI9A from Lyttelton volcano has distinctly higher FeO^t, alkalis, incompatible trace element concentrations (Figs 3 and 4b) and $^{206}Pb/^{204}Pb$, but lower $^{207}Pb/^{204}Pb$, compared with the Lyttelton shield-stage volcanic rocks. This suggests lower degrees of partial melting of a metasomatized peridotitic source component towards the end of the activity of the Lyttelton volcano (Figs 5 and 6). The high-silica Diamond Harbour lavas, erupted on the northern flank of the Lyttelton volcano, are transitional tholeiites ($SiO_2 \geq 48$ wt %) with high MgO (>8 wt %). These volcanic rocks have the highest Pb, U, and Th contents [resulting in low (Ce, Nd)/Pb, Nb/(U, Th)], together with the lowest Sr, TiO_2, CaO, FeO^t, $^{143}Nd/^{144}Nd$ and $^{206}Pb/^{204}Pb$ observed in Banks Peninsula volcanic rocks. These melts may, therefore, primarily represent partial melts from subduction-related pyroxenites, which may also have interacted with continental crustal material, contributing further to the high Pb, Th and U contents in these melts.

In conclusion, we propose that the high-silica Lyttelton melts primarily represent partial melts of pyroxenitic cumulates in the lithosphere, derived from Mt. Somers type arc melts during Gondwana subduction. These melts may have also interacted extensively with continental crustal material. It is also clear from the arrays formed by the combined Lyttelton and Akaroa data that extensive mixing occurred between asthenospheric and lithospheric melts. Although the Lyttelton volcanic rocks contain a greater lithospheric component and the Akaroa melts a greater asthenospheric component, melts from both asthenospheric and lithospheric sources appear to have been involved in forming both volcanic complexes.

DYNAMIC MODEL FOR THE MAGMATIC EVOLUTION OF BANKS PENINSULA

Recently Finn *et al.* (2005) and Hoernle *et al.* (2006) have pointed out the difficulties of explaining intraplate volcanism in the New Zealand area with either the mantle plume model or continental rifting. Hoernle *et al.* (2006) proposed lithospheric detachment to explain the intraplate volcanism in the Otago region, both for the Dunedin volcano and for the monogenetic volcanic fields such as the Waipiata Volcanic Field. We believe that lithospheric detachment/delamination is also an appropriate model for explaining the origin of the Banks Peninsula volcanism. To form the two volcanoes of the Banks Peninsula, we propose two delamination events. The first delamination event removed some of the subduction-modified lower lithosphere beneath Lyttelton volcano, causing upwelling of the upper asthenosphere (Fig. 12) and subsequent decompression melting (Fig. 13a). The asthenospheric melts triggered low-degree melting of the metasomatized, volatile-rich lithospheric mantle, containing pyroxenitic cumulates and frozen subduction-related Mt. Somers (±MBL dike) melts. The low-silica asthenospheric melts interacted extensively with the lithospheric melts. Lithospheric melting and interaction with asthenospheric melts are most likely during the initial stages of delamination, when there is extensive enriched lithosphere present, which has not yet been depleted by melting, and magma pathways to the surface are not yet well established. Melting of metasomatized (enriched) portions of the delaminated lithosphere may also have contributed to the Lyttelton volcanism (e.g. Elkins-Tanton, 2007).

After the formation of the Lyttelton volcano, another major delamination event occurred, removing most of the enriched lithosphere beneath Akaroa volcano (Fig. 13b). The more extensive delamination event beneath Akaroa volcano allowed more upwelling of the upper asthenosphere to shallower depths. This triggered more voluminous decompression partial melting, resulting in the formation of the much larger Akaroa volcano. The larger volumes of newly formed magma presumably ascended more rapidly through the thinner lithosphere beneath Akaroa volcano, and therefore experienced less lithospheric interaction than the Lyttelton group volcanic rocks. In addition, the greater volumes of asthenospheric melts would cause dilution of any lithospheric contaminants. In addition, the larger delamination event could have removed most of the enriched (subduction-modified) lithospheric mantle. Alternatively, the Banks magmatism may have resulted from a single delamination event that started beneath Lyttelton and propagated beneath the Akaroa volcano over the course of several million years. Two temporally separated voluminous pulses of volcanic

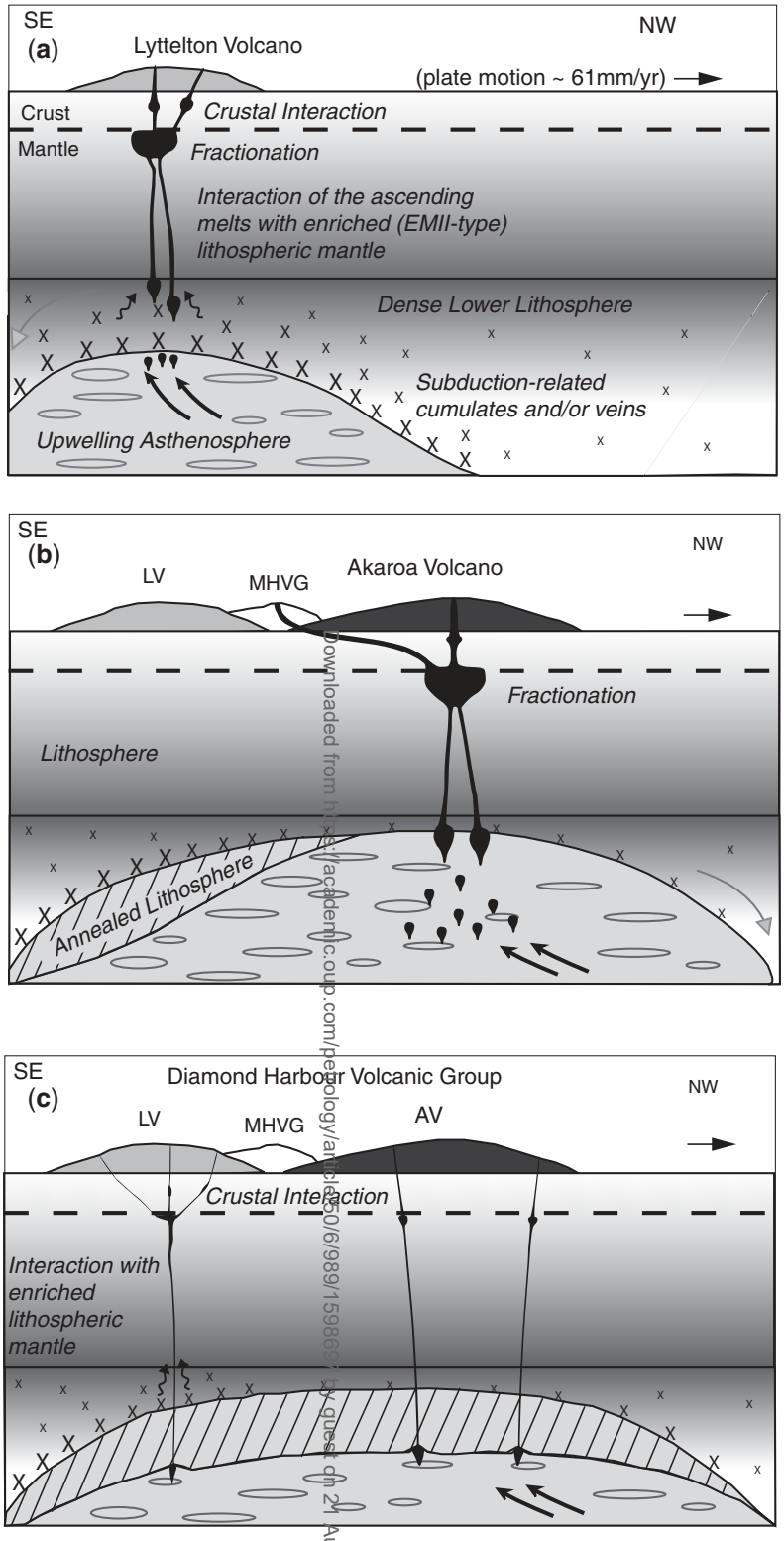

Fig. 13. (a–c) Schematic model to explain the development of intraplate volcanism at Banks Peninsula. As a result of prolonged exposure to subduction-related magmatic activity during the Palaeozoic and Mesozoic at the northern margin of Gondwana (bringing in fluids and melts) the lower lithosphere beneath Zealandia (and the Banks Peninsula) became enriched. Basaltic dikes, converted to eclogite, increased the density of the lower lithosphere with respect to the underlying asthenosphere. Therefore, this boundary represents a layer of gravitational instability, where the dense lower lithosphere is negatively buoyant. Detachment of the lower lithosphere results in upwelling of the less dense asthenospheric mantle into the resulting gap, partially melting as a result of decompression. A first detachment event occurred beneath Lyttelton volcano (a). Asthenospheric melts interacted with the enriched continental lithosphere (mantle and crust). A second, larger detachment event took place to the SW beneath the Akaroa volcano (b). Late-stage volcanism of the Diamond Harbour Volcanic Group formed by continued upwelling as the plate moved to the NW but annealed and thickened (c). The duration of late-stage volcanism suggests that it takes *c.* 1–3 Myr for the lithosphere to anneal completely and regain at least the thickness at which no further partial melting occurs after a detachment event.

activity, however, are more easily explained by two separate delamination/detachment events or two distinct stages of delamination.

During the late-stage volcanism, the low-degree, low-silica Diamond Harbour magmas ascended through the lithosphere beneath Akaroa volcano, undergoing minimum lithospheric interaction, possibly as a result of the presence of thinner lithosphere. On the other hand, the high-silica lavas erupted at Lyttelton volcano appear to represent interaction between low-silica partial melts derived from the asthenosphere and partial melts of the mantle lithosphere, previously enriched by subduction-related magmatism, and of the local crust (Fig. 13c).

There are a number of reasons why the relative lithospheric contribution to Lyttelton melts was greater than for Akaroa melts. Thinner lithosphere beneath Lyttelton volcano after the delamination event may have been one of the major factors causing greater lithospheric contamination of the Lyttelton asthenospheric melts. Interestingly, older crustal rocks are exposed at Lyttelton but not at Akaroa volcano, possibly suggesting a difference in the composition of the crust beneath the two volcanoes that may also in part be responsible for the greater observed lithospheric involvement at Lyttelton. It is possible, for example, that the crust beneath Akaroa is more mafic than that beneath Lyttelton and thus melts at a higher temperature, contributing less to crustal contamination than more silicic crust. Similarly the lithospheric mantle beneath Lyttelton volcano may also have had a different (more enriched) composition than that beneath Akaroa volcano, possibly reflecting local differences in lithospheric metasomatism/enrichment during subduction along the Gondwana margin.

In addition to the mafic magmas more evolved magmas (e.g. trachytes, rhyolites) were erupted contemporaneously with the mafic magmas at both volcanoes. This indicates that there were magma reservoirs beneath both Lyttelton and Akaroa volcanoes where magma was stored, fractionated and, depending on depth, may have assimilated crustal and/or mantle material (Fig. 13). Considering the duration of volcanism on Banks Peninsula, the entire process of lithospheric removal (detachment/delamination) must have occurred within <10 Myr. The prolonged late-stage volcanism at Akaroa volcano suggests an annealing time of the lower lithosphere of ~2–3 Myr (i.e. the time it takes the lithosphere to re-thicken) so that no further upwelling and melting occurs. Prolonged melt extraction out of the upper asthenospheric mantle will leave a more depleted peridotitic mantle residue (Jaupart, 2007), which presumably became a part of the lithospheric mantle beneath Banks Peninsula. Numerical modeling of lithospheric removal, which treats the lower lithosphere as a highly viscous fluid, reveals that the removal process is a large-scale feature producing cavities at the base of the lithosphere of the order of $\geq$100 km in length (e.g. Conrad & Molnar, 1996). However, these models do not include compositional changes or different rheologies along the base of the lithosphere, which may change the physical behavior of the lower lithosphere.

Finally, geophysical investigations of Cenozoic deformation rates as a result of clockwise rotation of the Pacific Plate have demonstrated increased structural deformation in the early to late Miocene (25–8 Ma; Hall *et al.*, 2004). This could have caused mild extension beneath Banks Peninsula in addition to the process of lithospheric detachment and hence resulted in increased melt productivity to form large intraplate volcanoes such as those on Banks Peninsula, the Dunedin volcano and Auckland and Campbell Island volcanoes, which formed during the Miocene.

CONCLUSION

New $^{40}Ar/^{39}Ar$ ages provide additional constraints on the temporal evolution of Tertiary volcanism on Banks Peninsula and indicate that activity initiated at ~12 Ma and persisted until ~7 Ma. The two large shield volcanoes, Lyttelton and Akaroa, both formed within ~1 Myr (Lyttelton ~12·3–11·5 Ma and Akaroa ~9·6–8·6 Ma) and each volcano had a period of late-stage volcanic activity persisting for 1–2·5 Myr.

Mafic (MgO > 4 wt %) intraplate volcanism on the Banks Peninsula, consisting of the Lyttelton volcano in the NW and the Akaroa volcano in the SE, can be divided into a low-silica group (SiO_2 < ~48 wt %), primarily occurring at the Akaroa volcano, and a high-silica group (SiO_2 > ~48 wt %), restricted to the Lyttelton volcano, with each group displaying distinct geochemical characteristics. All the mafic volcanic rocks of the Banks Peninsula show ocean island basalt incompatible element patterns on multi-element diagrams; however, the low-silica Akaroa group lavas are characterized by more pronounced positive Nb, Ta and negative Pb anomalies, compared with the high-silica Lyttelton volcanic rocks. Compared with the high-silica mafic Lyttelton lavas, the low-silica mafic Akaroa lavas also have high contents of TiO_2, FeO^t, CaO, Nb and Sr; high ratios of Zr/Hf, Sr/Y, (La, Sm)/Yb, (Ce, Nd)/Pb and (Nb, Ta)/(U, Th, Ba, Rb, La); and more radiogenic Pb, Nd and Hf and less radiogenic Sr isotopic compositions. Compared with N-MORB, the low-silica Akaroa lavas have more radiogenic Pb and Sr and less radiogenic Nd and Hf isotopic compositions, which are consistent with the influence of recycled oceanic lithosphere in the source of these lavas.

Our modelling shows that the Akaroa isotopic compositions could be explained by a mixture of approximately 8–20% of ~0·7–1·3 Ga recycled oceanic lithosphere, as carbonated eclogite, with peridotite. We propose that the carbonated eclogite resided in a depleted peridotitic

matrix. Upon upwelling, the carbonated eclogite partially melted at a depth ≥180 km and these melts metasomatized the surrounding peridotitic asthenosphere in the upwelling melting column. At depths of ~110 km, the carbonated peridotite crosses its solidus and melts to form the low-silica Akaroa melts.

The high-silica group lavas, in contrast, have generally lower contents of FeO^t, TiO_2, CaO (and low peridotite/pyroxenite index) and incompatible elements (e.g. Sr, Nb, etc.); and lower (Ce, Nd)/Pb, Nd/La, Nb/Th and Nb/U ratios. The geochemistry of these melts can be best explained through mixing of asthenospheric melts with melts of EMII-type pyroxenitic cumulates in the lithosphere, formed during subduction along the Gondwana margin, and crustal interaction.

Because there are no morphological and geophysical indications of a thermal anomaly and/or of major lithospheric extension beneath the Banks Peninsula, we propose lithospheric removal (detachment/delamination) to explain the magmatic activity. To form the Lyttelton and Akaroa volcanoes, two detachment events or a two-stage delamination event are required. An initial detachment event caused upwelling of the heterogeneous asthenospheric mantle (containing recycled oceanic crust), resulting in decompression melting. The upwelling mantle and rise of asthenospheric melts triggered melting of pyroxenitic cumulates and crustal rocks in the lithosphere, which formed the Lyttelton volcano. A second, larger detachment event, or larger, second phase of delamination, caused greater upwelling, resulting in more voluminous generation of low-silica asthenospheric melts. These greater volumes of asthenospheric melts reached the surface with minimal lithospheric interaction and formed the larger Akaroa volcano.

ACKNOWLEDGEMENTS

We would like to thank F. Hauff, D. Rau, J. Sticklus, S. Hauff and J. Fietzke for analytical and technical assistance, J. White for help with the field work, M. Portnyagin for fruitful discussions, and J. Davidson and K. Knesel for constructive reviews of the manuscript. This project was partially funded by the German Research Foundation (DFG, project HO1833/12-1). All analytical work conducted at IFM-GEOMAR, however, was funded by IFM-GEOMAR.

SUPPLEMENTARY DATA

Supplementary data for this paper are available at *Journal of Petrology* online.

REFERENCES

Barley, M. E. & Weaver, S. D. (1988). Strontium isotope composition and geochronology of intermediate–silicic volcanics, Mt Somers and Banks Peninsula, New Zealand. *New Zealand Journal of Geology and Geophysics* **31**, 197–206.

Bindeman, I. N., Eiler, J. M., Yogodzinski, G. M., Tatsumi, Y., Sterne, C. R., Grove, T. L., Portnyagin, M., Hoernle, K. & Danyushevsky, L. V. (2005). Oxygen isotope evidence for slab melting in modern and ancient subduction zones. *Earth and Planetary Science Letters* **235**, 480–496.

Blichert-Toft, J., Chauvel, C. & Albarède, F. (1997). Separation of Hf and Lu for high-precision isotope analyses of rock samples by magnetic sector-mutiple collector ICP-MS. *Contributions to Mineralogy and Petrology* **127**, 248–260.

Blichert-Toft J, Albarede F (1997) The Lu-Hf isotope geochemistry of chondrites and the evolution of the mantle-crust system. *Earth and Planetary Science Letters* **148**, 243–258.

Bohrson, W. A. & Spera, F. J. (2001). Energy-constrained open-system magmatic processes II: Application of energy-constrained assimilation–fractional crystallization (EC-AFC) model to magmatic systems. *Journal of Petrology* **42**, 1019–1041.

Clouard, V. & Bonneville, A. (2005). Ages of seamounts, islands and plateaus and plateaus on the Pacific plate. In: Foulger, G. R., Natland, J. H., Presnall, D. C. & Anderson, D. L. (eds) *Plates, Plumes, and Paradigms. Geological Society of America, Special Papers* **388**, 71–90.

Conrad CP, Molnar P (1996). The growth of Rayleigh-Taylor instabilities in the lithosphere for various rheological and density structures. *Geophysical Journal International* **129**, 95–112.

Coombs, D. S., Cas, R. A., Kawachi, Y., Landis, C. A., McDonough, W. F. & Reay, A. (1986). Cenozoic Volcanism in North, East and Central Otago. In: Smith, I. E. M. (ed.) *Cenozoic Volcanism in New Zealand*. Wellington, Royal Society of New Zealand, pp. 278–312.

Dasgupta, R., Hirschmann, M. M. & Stalker, K. (2006). Immiscible transition from carbonate-rich to silicate-rich melts in the 3 GPa melting interval of eclogite + CO_2 and genesis of silica-undersaturated ocean island lavas. *Journal of Petrology* **47**, 647–671.

Dasgupta, R., Hirschmann, M. M. & Smith, N. (2007*a*). Partial melting experiments of peridotite ± CO_2 at 3 GPa and genesis of alkalic ocean island basalts. *Journal of Petrology* **48**, 2093–2124.

Dasgupta, R., Hirschmann, M. M. & Smith, N. (2007*b*). Water follows carbon: CO_2 incites deep silicate melting and dehydration beneath mid-ocean ridges. *Geology* **35**, 135–138, doi:10.1130/G22856A.

Davy, B. (2006). Bollons Seamount and early New Zealand–Antarctic seafloor spreading. *Geochemistry, Geophysics, Geosystems* **7**, Q06021, doi:10.1029/2005GC001191.

Downes H (2007) Origin and significance of spinel and garnet pyroxenites in the shallow lithospheric mantle: Ultramafic massifs in orogenic belts in Western Europe and NW Africa. *Lithos* **99**, 1–24.

Duffield, W. A. & Dalrymple, G.B. (1990). The Taylor Creek Rhyolite of New Mexico: a rapidly emplaced field of lava domes and flows. *Bulletin of Volcanology* **52**, 475–487.

Eberhart-Phillips, D. & Bannister, S. (2002). Three-dimensional crustal structure in the Southern Alps region of New Zealand from inversion of local earthquake and active source data. *Journal of Geophysical Research* **107**, doi:10.1029/2001JB000567.

Eiler JM (2001) Oxygen isotope variations of basaltic lavas and upper mantle rocks. *Reviews in Mineralogy and Geochemistry* **43**, 319–364.

Elkins, L. J. (2008). Partitioning of U and Th during garnet pyroxenite partial melting: constraints on the source of alkaline ocean island basalts. *Earth and Planetary Science Letters* **265**, 270–286.

Elkins-Tanton, L. T. (2007). Continental magmatism, volatile recycling, and heterogeneous mantle caused by lithospheric gravitational instabilities. *Journal of Geophysical Research* **112**, B03405, doi:10.1029/2005JB004072.

Finn, C. A., Mueller, R. D. & Panter, K. S. (2005). A Cenozoic diffuse alkaline magmatic province (DAMP) in the southwest Pacific without rift or plume origin. *Geochemistry, Geophysics, Geosystems* **6**, Q02005, doi:10.1029/2004GC000723.

Garbe-Schönberg, C.-D. (1993). Simultaneous determination of thirty-seven trace elements in twenty-eight international rock standards by ICP-MS. *Geostandards Newsletter* **17**, 81–97.

Geldmacher, J. & Hoernle, K. (2000). The 72 Ma geochemical evolution of the Madeira Hotspot (eastern North Atlantic): recycling of Palaeozoic (≤500 Ma) basaltic and gabbroic crust. *Earth and Planetary Science Letters* **183**, 73–92 [Corrigendum in **186**, 333 (2001)].

Govindaraju, K. (1994). Compilation of working values and sample description for 383 geostandards. *Geostandards Newsletter* **18**, 1–158.

Gurenko, A. A., Sobolev, A. V., Hoernle, K. A., Hauff, F. & Schmincke, H. U. (2008). Enriched, HIMU-type peridotite and depleted recycled pyroxenite in the Canary plume: A mixed-up mantle. *Earth and Planetary Science Letters* doi:10.1016/j.epsl.2008.11.013.

Hall, L. S., Lamb, S. H. & Mac Niocaill, C. (2004). Cenozoic distributed rotational deformation, South Island, New Zealand. *Tectonics* **23**, 1–16.

Hansteen, T. H. & Troll, V. R. (2003). Oxygen isotope composition of xenoliths from the oceanic crust and volcanic edifice beneath Gran Canaria (Canary Islands): consequences for crustal contamination of ascending magmas. *Earth and Planetary Science Letters* **193**, 181–193.

Harmon, R. S. & Hoefs, J. (1995). Oxygen isotopes heterogeneity of the mantle deduced from global ^{18}O systematics of basalts from different tectonic settings. *Contributions to Mineralogy and Petrology* **120**, 95–114.

Herzberg, C. (2006*a*). Petrology and thermal structure of the Hawaiian plume from 744 Mauna Kea volcano. *Nature* **444**, 605–609.

Herzberg, C. (2006*b*). Distribution and size of pyroxenite bodies in the mantle. *EOS Transactions, American Geophysical Union* **746**, Fall Meeting Supplement, Abstract U12A-04.

Herzberg, C. & Asimow, P. D. (2008). Petrology of some oceanic island basalts: PRIMELT2.XLS software for primary magma calculation. *Geochemistry, Geophysics, Geosystystems* **9**, Q09001, doi:10.1029/2008GC002057.

Herzberg, C., Asimow, P. D., Arndt, N., Niu, Y., Lesher, C. M., Fitton, J. G., Cheadle, M. J. & Saunders, A. D. (2007). Temperatures in ambient mantle and plumes: Constraints from basalts, picrites, and komatiites. *Geochemistry, Geophysics, Geosystystems* **8**, Q02006, doi:10.1029/2006GC001390.

Hirose, K. & Kushiro, I. (1993). Partial melting of dry peridotites at high pressures: Determination of compositions of melts segregated from peridotite using aggregates of diamond. *Earth and Planetary Science Letters* **114**, 477–489.

Hirose K (1997) Partial melt compositions of carbonated peridotite at 3 GPa and role of CO2 in alkali-basalt magma generation. *Geophysical Research Letters* **24**, 2837–2840.

Hirschmann, M. M., Kogiso, T., Baker, M. B. & Stolper, E. M. (2003). Alkalic magmas generated by partial melting of garnet pyroxenite. *Geology* **31**, 481–484.

Hoernle, K., Tilton, G. & Schmincke, H.-U. (1991). Sr–Nd–Pb isotopic evolution of Gran Canaria: evidence for shallow enriched mantle beneath the Canary Islands. *Earth and Planetary Science Letters* **106**, 44–63.

Hoernle K (1998) Geochemistry of Jurassic oceanic crust beneath Gran Canaria (Canary Islands): Implications for crustal recycling and assimilation. *Journal of Petrology* **39**, 859–880.

Hoernle K., White J. D. L., Bogaard P. V. D., Hauff F., Coombs D. S., Werner R., Timm C., Garbe-Schönberg D., Reay A. & Cooper A. F. (2006) Cenozoic Intraplate Volcanism on New Zealand: Upwelling Induced by Lithospheric Removal. *Earth and Planetary Science Letters* **248**, 335–352.

Hoernle, K., Abt, D. L., Fischer, K. M., Nichols, H., Hauff, F., Abers, G. A., van den Bogaard, P., Heydolph, K., Alvarado, G., Protti, M. & Strauch, W. (2008). Arc-parallel flow in the mantle wedge beneath Costa Rica and Nicaragua. *Nature* doi:10.1038/nature06550.

Hofmann, A. W. (1988). Chemical differentiation of the Earth: the relationship between mantle, continental and oceanic crust. *Earth and Planetary Science Letters* **90**, 297–314.

Hofmann, A. W. (2006). Lead in oceanic basalts and the mantle—20 years later. *Geophysical Research Abstracts* **8**, 10305.

Hofmann, A. W. & White, W. M. (1982). Mantle plumes from ancient oceanic crust. *Earth and Planetary Science Letters* **79**, 33–45.

Hofmann, A. W., Jochum, K., Seufert, M. & White, W. M. (1986). Nb and Pb in oceanic basalts: new constraints on mantle evolution. *Earth and Planetary Science Letters* **57**, 421–436.

Jaupart, C. (2007). Dynamics of continental lithosphere. *Geophysical Research Abstracts* **9**, 06818, SRef-ID: 1607–7962/gra/EGU2007-A-06818.

John, T., Scherer, E. E., Haase, K. & Schenk, V. (2004). Trace element fractionation during fluid-induced eclogitization in a subducting slab: trace element and Lu–Hf–Sm–Nd isotope systematics. *Earth and Planetary Science Letters* **227**, 441–456.

Kogiso, T. & Hirschmann, M. M. (2006). Partial melting experiments of bimineralic eclogite and the role of recycled mafic oceanic crust in the genesis of ocean island basalts. *Earth and Planetary Science Letters* **249**, 188–199.

Liggett, K. A. & Gregg, D. R. (1965). Geology of Banks Peninsula, South Island—Tour D. In: Kermode, L. O. (ed.) *New Zealand Volcanology—South Island. Department of Scientific and Industrial Research Information Series* **51**, 9–25.

Liu, Z. & Bird, P. (2006). Two-dimensional and three-dimensional finite element modelling of mantle processes beneath central South Island, New Zealand. *Geophysical Journal International* **365**, 1003–1028.

Lundstrom, C. C., Hoernle, K. & Gill, J. (2003). U-series disequilibria in volcanic rocks from the Canary Islands: Plume versus lithospheric melting. *Geochimica et Cosmochimica Acta* **67**, 4153–4177, doi:10.1016/S0016-7037(03)00308-9.

Mattey, D., Lowry, D. & McPherson, C. (1994). Oxygen isotope composition of mantle peridotite. *Earth and Planetary Science Letters* **128**, 231–241.

Montelli, R., Nolet, G., Dahlen, R. A. & Masters, G. (2006). A catalogue of deep mantle plumes: New results from finite frequency tomography. *Geochemistry, Geophysics, Geosystems* **7**, Q11007, doi:10.1029/2006GC001248.

Morgan, W. J. (1971). Convection plumes in the lower mantle. *Nature* **230**, 42–43.

Muir, R. J., Ireland, T. R., Weaver, S. D., Bradshaw, J. D., Evans, J. A., Eby, G. N. & Shelley, D. (1998). Geochronology and geochemistry of a Mesozoic magmatic arc system, Fjordland, New Zealand. *Journal of the Geological Society, London* **155**, 1037–1053.

Panter, K. S., Blusztain, J., Hart, S. R., Kyle, P. R., Esser, R. & McIntosh, W. C. (2006). The origin of HIMU in the SW Pacific: evidence from interplate volcanism in southern New Zealand and subantarctic islands. *Journal of Petrology* **47**, 1–32, doi:10.1093/petrology/egl024.

Pertermann, M. & Hirschmann, M. M. (2002). Trace-element partitioning between vacancy-rich eclogitic clinopyroxene and silicate melt. *American Mineralogist* **87**, 1365–1376.

Pfänder, J. A., Münker, C., Stracke, A. & Mezger, K. (2007). Nb/Ta and Zr/Hf in ocean island basalts—implications for crust–mantle differentiation and the fate of niobium. *Earth and Planetary Science Letters* **254**, 158–172.

Pilet, S., Baker, M. B. & Stolper, E. M. (2008). Metasomatized lithosphere and the origin of alkaline lavas. *Science* **320**, doi:10.1126/science.1156563.

Rudnick, R. L., Barth, M., Horn, I. & McDonough, W. F. (2000). Rutile-bearing refractory eclogites: missing link between continents and depleted mantle. *Science* **287**, 278–281.

Schmidt, M. W., Dardon, A., Chazot, G. & Vannucci, R. (2004). The dependence of Nb and Ta rutile–melt partitioning on melt composition and Nb/Ta fractioning during subduction processes. *Earth and Planetary Science Letters* **226**, 415–432.

Sewell, R. J. (1988). Late Miocene volcanic stratigraphy of central Banks Peninsula, Canterbury, New Zealand. *New Zealand Journal of Geology and Geophysics* **31**, 41–64.

Sewell, R. J., Weaver, S. D. & Reay, M. B. (1992). *Geology of Banks Peninsula Scale 1:100,000*. Lower Hutt, New Zealand: Institute of Geological & Nuclear Sciences, Geological Map **3**.

Shelley, D. (1988). Radial dikes of Lyttelton Volcano—their structure, form and petrography. *New Zealand Journal of Geology and Geophysics* **31**, 65–75.

Sobolev, A. V., Hofmann, A. W., Sobolev, S. V. & Nikogosian, I. K. (2005). An olivine free mantle source of Hawaiian shield basalts. *Nature* **434**, 590–597.

Sobolev, A. V., Hofmann, A. W., Kuzmin, D. V., Yaxley, G. M., Arndt, N. T., Chung, S.-L., Danyushevsky, L. V., Elliott, T., Frey, F. A., Garcia, M. O., Gurenko, A. A., Kamenetsky, V. S., Kerr, A. C., Krivolutskaya, N. A., Matvienkov, V. V., Nikogosian, I. K., Rocholl, A., Sigurdsson, I. A., Sushchevskaya, N. M. & Teklay, M. (2007). The amount of recycled crust in sources of mantle-derived melts. *Science* doi:10.1126/science.1138113.

Spera, F. J. & Bohrson, W. A. (2001). Energy-constrained open-system magmatic processes I: General model and energy-constrained assimilation and fractional crystallization (EC-AFC) formulation. *Journal of Petrology* **42**, 999–1018.

Sprung, P., Schuth, S., Münker, C. & Hoke, L. (2007). Intraplate volcanism in New Zealand: the role of fossil plume material and variable lithospheric properties. *Contributions to Mineralogy and Petrology* **153**, 669–687.

Stern, T., Okaya, D. & Scherwath, M. (2002). Structure and strength of a continental transform from onshore–offshore seismic profiling of South Island, New Zealand. *Earth, Planets, Space* **54**, 1011–1019.

Stipp, J. J. & Mc Dougall, I. (1968). Geochronology of the Banks Peninsula volcanoes, New Zealand. *New Zealand Journal of Geology and Geophysics* **11**, 1239–1260.

Sun S-s & McDonough W F (1989). Chemical and isotopic systematics of oceanic basalts: implications for mantle composition and processes. In: Saunders, A. D. & Norry, M. J. (eds) *Magmatism in the Ocean Basins. Geological Society, London, Special Publications* **42**, 313–345.

Sutherland, R. (1995). The Australia–Pacific boundary and Cenozoic plate motions in the SW Pazific: Some constraints from Geosat data. *Tectonics* **14**, 819–831.

Tappenden, V. (2003). Magmatic response to the evolving New Zealand Margin of Gondwana during the Mid–Late Cretaceous. PhD thesis, University of Canterbury, New Zealand, 261 pp.

Todt, W., Cliff, R. A., Hanser, A. & Hofmann, A. W. (1996). $^{202}Pb + ^{205}Pb$ double spike for lead isotopic analyses. In: Basu, A. & Hart, S. (eds) *Earth Processes: Reading the Isotopic Code. Geophysical Monograph, American Geophysical Union* **95**, 429–437.

Turner, S., Tonarini, S., Bindeman, I., Leeman, W. P. & Schaefer, B. F. (2007). Boron and oxygen isotope evidence for recycling of subducted components over the past 2·5 Gyr. *Nature* **447**, doi:10.1038/nature05898.

van den Bogaard, P. (1995). $^{40}Ar/^{39}Ar$ ages of sanidine phenocrysts from Laacher See tephra (12,900 yr BP): chronostratigraphic and petrological significance. *Earth and Planetary Science Letters* **133**, 163–174.

Waight, T. E., Weaver, S. D. & Muir, R. J. (1998). Mid-Cretaceous granitic magmatism during the transition from subduction to extension in southern New Zealand: a chemical and tectonic synthesis. *Lithos* **45**, 469–482.

Weaver, B. L. (1991). The origin of ocean island basalt end-member compositions: trace element and isotopic constraints. *Earth and Planetary Science Letters* **104**, 381–397.

Weaver, S. D. & Sewell, R. J. (1986). Cenozoic volcanic geology of the Banks Peninsula. South Island igneous rocks. In: Houghton, B. F. & Weaver, S. D. (eds) *New Zealand Geological Survey Record* **13**, 39–63.

Weaver, S. D. & Smith, I. E. M. (1989). New Zealand intraplate volcanism. In: Johnson, R. W., Knutson, J. & Taylor, S. R. (eds) *Intraplate Volcanism in Eastern Australia and New Zealand*. Cambridge: Cambridge University Press, pp. 157–188.

Workman, R. K. & Hart, S. R. (2005). Major and trace element composition of the depleted MORB mantle (DMM). *Earth and Planetary Science Letters* **231**, 53–72.

Yaxley, G. M. & Green, D. H. (1994). Experimental demonstration of refractory carbonate-bearing eclogite siliceous melt in the subduction regime. *Earth and Planetary Science Letters* **128**, 313–325.

Zindler A, and Hart S (1986) Chemical Geodynamics. *Annual Review of Earth and Planetary Sciences* **14**, 493–571.